Design and synthesis of novel 8-(azaindolyl)-benzoazepinones as potent and selective ROCK inhibitors

Daniele Pala,[a*] David Clark,[b] Christine Edwards,[b] Elisa Pasqua,[b] Laura Tigli,[a] Barbara Pioselli,[a] Piotr Malysa,[c] Fabrizio Facchinetti,[a] Fabio Rancati [a] and Alessandro Accetta [a*]

[a] *Global Research and Preclinical Development, Chiesi Farmaceutici S.p.A, Parma 43122, Italy.*
[b] *Charles River Laboratories, 8–9 Spire Green Centre, Harlow CM19 5TR, UK.*
[c] *Chemistry Department, Selvita S.A., Kraków, Poland.*
**Corresponding authors* (d.pala@chiesi.com, a.accetta@chiesi.com).

Index

1. Molecular Modelling/Virtual Screening Campaign

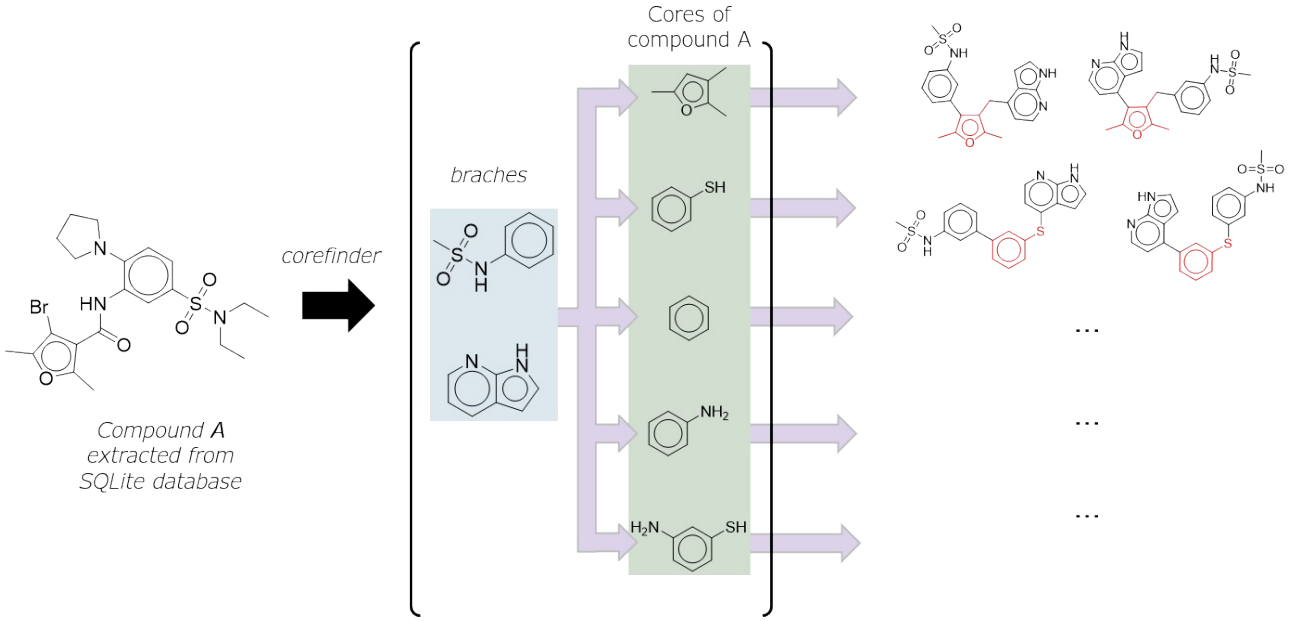

Figure S1. Schematic representation of the linking procedure. The *corefinder* utility was first applied on a compound **A** retrieved from the original SQLite database (left). Each core identified by the *corefinder* utility (green) was then linked to the terminal *branches* extracted from the co-crystallized ROCK ligand (light blue). Specifically, each linking combination between the core and the branches was generated and included in the final compound dataset (right).

2. HDX-MS

Table S1. HDX-MS data summary.

Data Set	**ROCK2**
HDX reaction details	10 mM phosphate in D_2O pD = 7.40 25 °C
HDX time course (min)	0.17, 0.50, 5, 10, 30, 60
HDX control samples	Maximally-labeled controls were not performed.
Back-exchange (mean / IQR)	N/A
# of Peptides	79
Sequence coverage (%)	90.98
Average peptide length / Redundancy	11.32 / 2.46
Replicates (biological or technical)	4 (technical)
Repeatability	0.123 (average SD)
Significant differences in HDX (delta HDX > X D)	0.60 (99% CI)

Figure S2a-d. ROCK2 deuterium uptake plots.

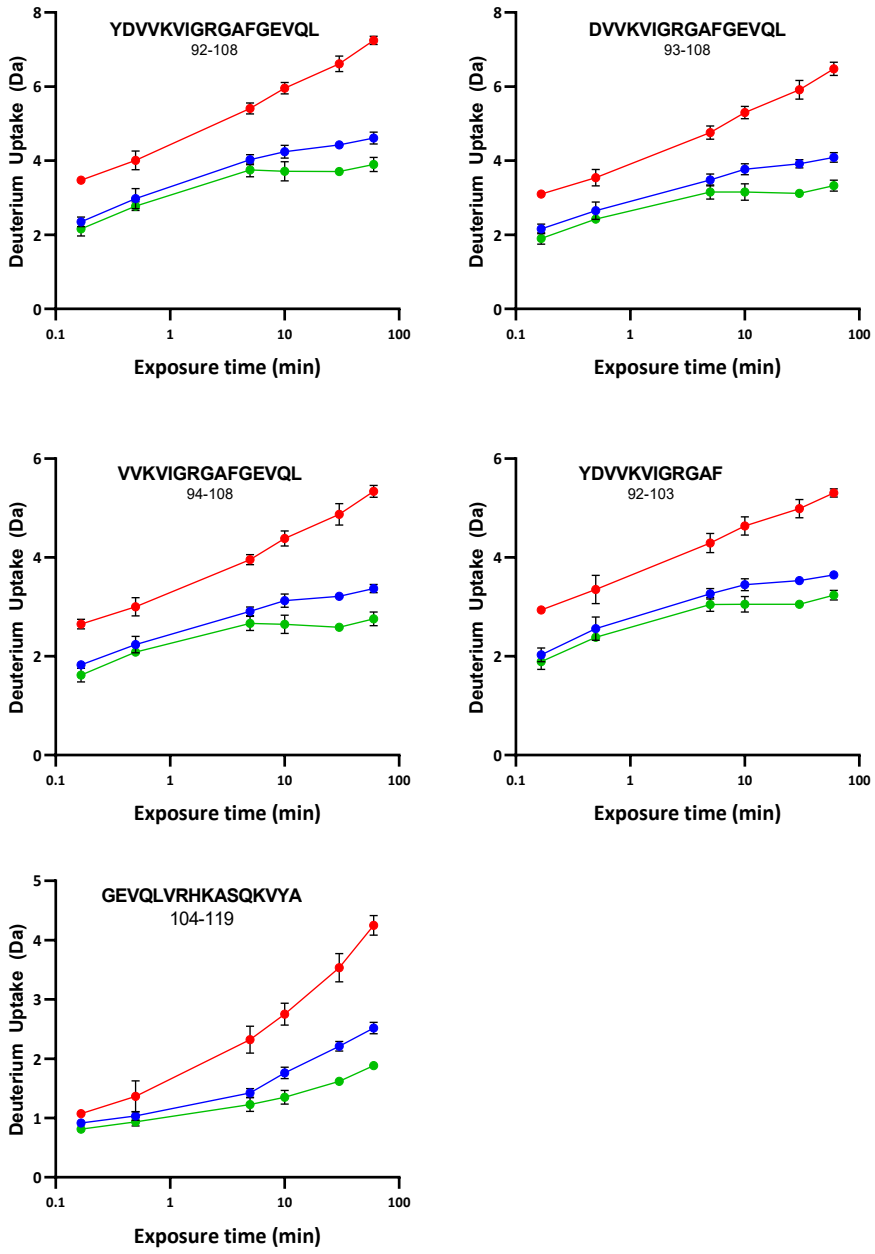

(**S2-a**) Deuterium uptake plots of redundant peptides belonging to ROCK2 glycine-rich loop. ROCK2 unbound kinetics in red, ROCK2-@**4** in blue, ROCK2-@**15** in green.

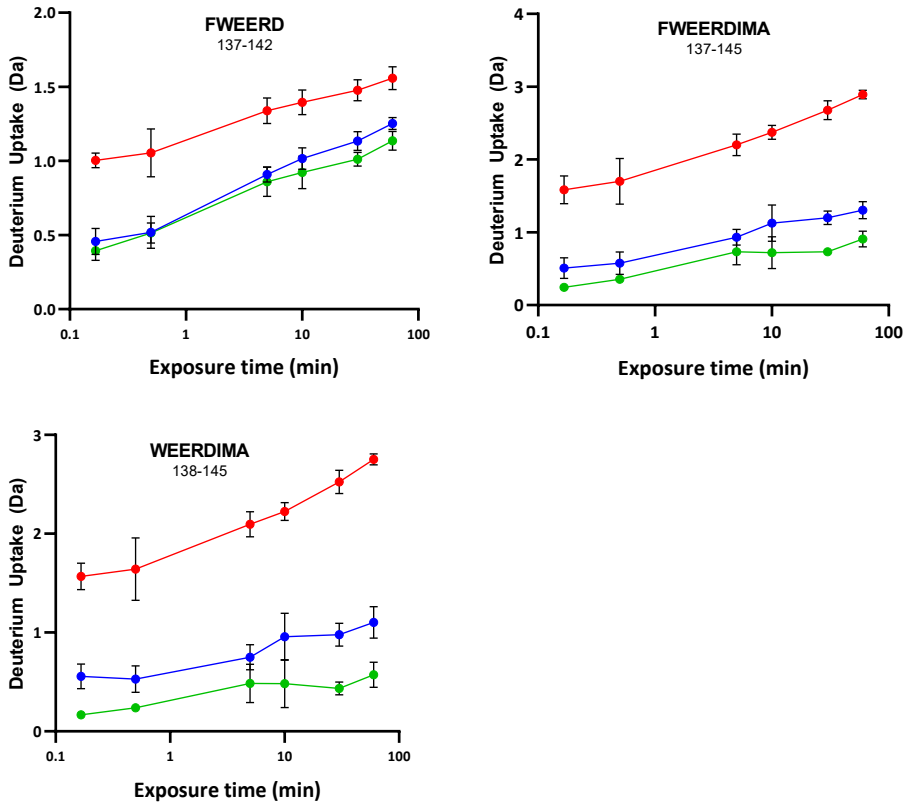

(**S2-b**) Deuterium uptake plots of redundant peptides belonging to ROCK2 α-helix C. ROCK2 unbound kinetics in red, ROCK2-@**4** in blue, ROCK2-@**15** in green.

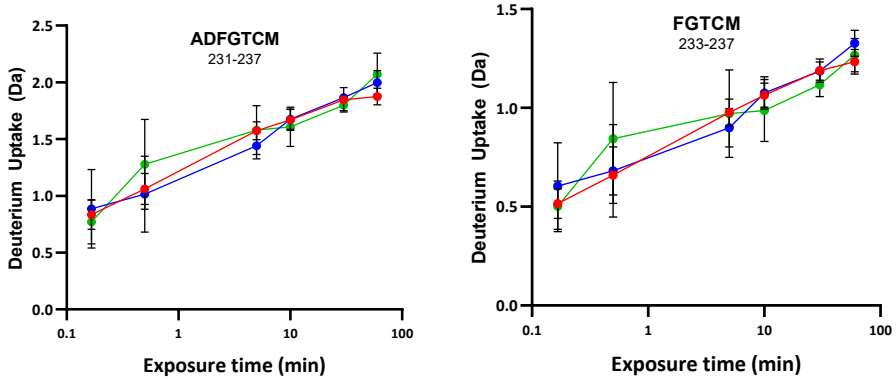

(**S2-c**) Deuterium uptake plots of redundant peptides belonging to ROCK2 activation loop. ROCK2 unbound kinetics in red, ROCK2-@**4** in blue, ROCK2-@**15** in green.

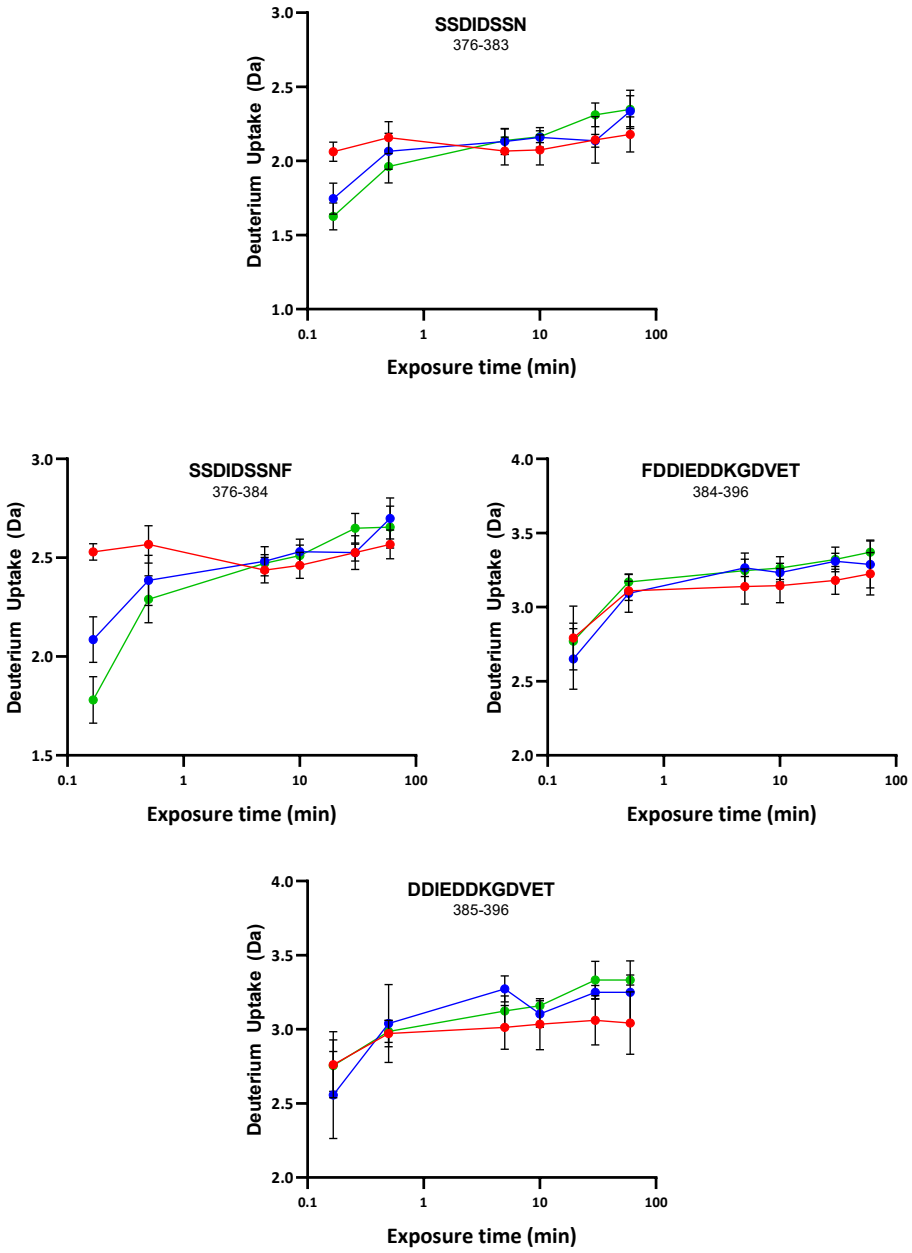

(**S2-d**) Deuterium uptake plots of redundant peptides belonging to ROCK2 C-tail. ROCK2 unbound kinetics in red, ROCK2-@**4** in blue, ROCK2-@**15** in green.

Figure S3. Statistical evaluation of differential deuterium uptakes.

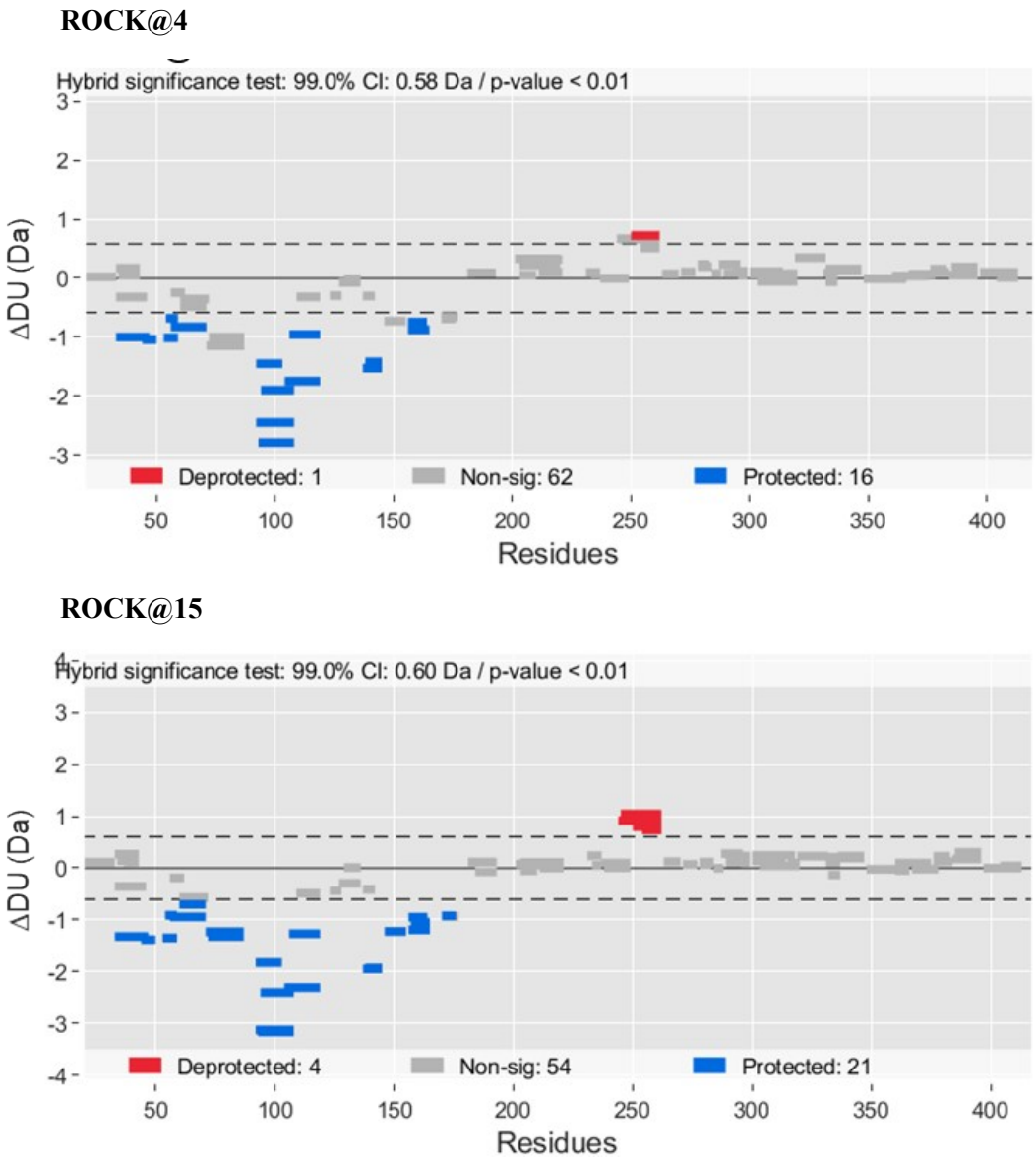

Wood's differential plot with hybrid statistical evaluation for ROCK2-@**4** (upper panel) and ROCK2-@**15** (lower panel) (Deuteros 2.0). Each bar represents an individual peptide, with bar length corresponding to peptide length. Red and blue colored bars indicate statistically significant deprotected or protected peptides, respectively, determined using a 99% confidence interval (dotted line). Peptides with no significant difference between conditions, are shown in grey. 60-minutes timepoint results are reported as an example, however peptides spanning the Glycine-rich loop and α-Helix C show significant protection also at earlier timepoints. Glycine-rich loop: 92-110; α-Helix C: 137-155; Activation loop: 231-242; C-tail: 376-402.

3. X-ray structure of ROCK1 co-crystallized with compound 2

Figure S4. X-ray structure (PDB ID: 5KKS) of ROCK1 (gray cartoons and sticks) co-crystallized with compound 2 (orange carbons). H-bond interactions are depicted with dashed black lines

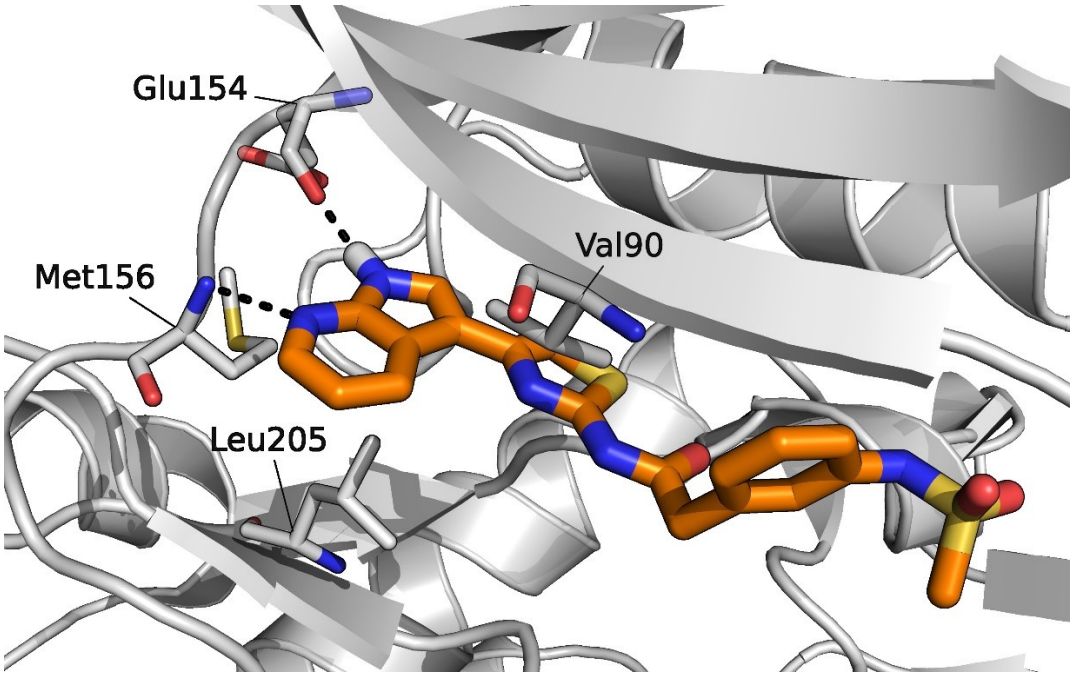

4. In-vitro Assays protocols

In vitro inhibitory activity assay description ROCK1 and ROCK2

The effectiveness of compounds to inhibit Rho kinase activity was determined in a 10 µL assay containing 40 mM Tris pH7.5, 20 mM $MgCl_2$ 0.1mg/mL BSA, 50 µM DTT and 2.5 µM peptide substrate (Myelin Basic Protein) using an ADP-Glo kit (Promega). Compounds were dissolved in DMSO such that the final concentration of DMSO was 1% in the assay. All reactions/incubations were performed at 25°C. Compound (2 □l) and either Rho kinase 1 or 2 (4 µL) were mixed and incubated for 30 min. Reactions were initiated by the addition of ATP (4 µL) such that the final concentration of ATP in the assay was 10 µM (***Low ATP protocol***) or 200 µM (***High ATP protocol***). After a 1 hour incubation, 10 µL of ADP-Glo Reagent was added and, after a further one hour incubation, 20 µL of Kinase Detection Buffer was added and the mixture incubated for a further 45 min. The luminescent signal was measured on a luminometer. Controls consisted of assay wells that did not contain compound with background determined using assay wells with no enzyme added. Compounds were tested in dose-response format and the inhibition of kinase activity was calculated at each concentration of compound. To determine the IC_{50} value (concentration of compound required to inhibit 50% of the enzyme activity), data were fit to a plot of % inhibition vs Log_{10} compound concentration using a sigmoidal fit with a variable slope and fixing the maximum to 100% and the minimum to 0%. To determine the Ki values the Cheng-Prusoff equation was utilized ($Ki = IC_{50}/(1 + [S]/Km)$.

In vitro inhibitory activity assay description for PKA

The effectiveness of compounds to inhibit PKA activity was determined in a 10 µL assay containing 40 mM Tris pH7.5, 20 mM $MgCl_2$ 0.1 mg/mL BSA, 50 µM DTT and 260 µM peptide substrate (kemptide) using an ADP-Glo kit (Promega). Compounds were dissolved in DMSO such that the final concentration of DMSO was 1% in the assay. All reactions/incubations were performed at 25°C. Compound and PKA enzyme (6 µL) were mixed and incubated for 30 min. Reactions were initiated by addition of ATP (4 µL) such that the final concentration of ATP in the assay was 10 µM. After a 30-minute incubation, 10 µL of ADP-Glo Reagent was added and, after a further 1 hour incubation, 20 µL of Kinase Detection Buffer was added and the mixture incubated for a further 45 min. The luminescent signal was measured on a luminometer. Controls consisted of assay wells that did not contain compound with background determined using assay wells with no enzyme added. Compounds were tested in dose-response format and the inhibition of kinase activity was calculated at each concentration of compound. To determine the IC_{50} value (concentration of compound required to inhibit 50% of the enzyme activity), data were fit to a plot of % inhibition vs Log_{10} compound concentration using a sigmoidal fit with a variable slope and fixing the maximum to 100% and the minimum to 0%. To determine the Ki values the Cheng-Prusoff equation was utilized ($Ki = IC_{50}/(1 + [S]/Km)$.

Phospho-MLC cellular inhibitory activity assay description

Human PASMC cells were seeded at 5000 cells per well in a 384 well plate and incubated with test compound for one hour, lysed and then levels of pMLC2 assessed using MSD plate technology. MSD plates were supplied pre-coated with anti-rabbit Ig. After blocking, plates were coated with anti-phospho MLC2 (rabbit) capture antibody, then washed before the addition of cell lysate, and incubated overnight at 4°C. Plates were then washed; an anti-MLC2 detection antibody (mouse) added followed by an anti-mouse-Ig-Sulpho-tag secondary antibody. The resulting signal was read on a Mesoscale Sector S 600 machine and was proportional to the levels of pMLC2 present in the cell lysate. Data are fitted by a four-parameter logistic dose-response curve using IDBS XLFit 4.2 Model 205.

4. ^{1}H-NMR and LC-MS traces of compounds 3 to 15

N-(3-(2-oxo-8-(1H-pyrrolo[2,3-b]pyridin-4-yl)-1,2,4,5-tetrahydro-3H-benzo[d]azepin-3-yl)phenyl)methanesulfonamide (3).

^{1}H NMR (300 MHz, DMSO-*d6*)

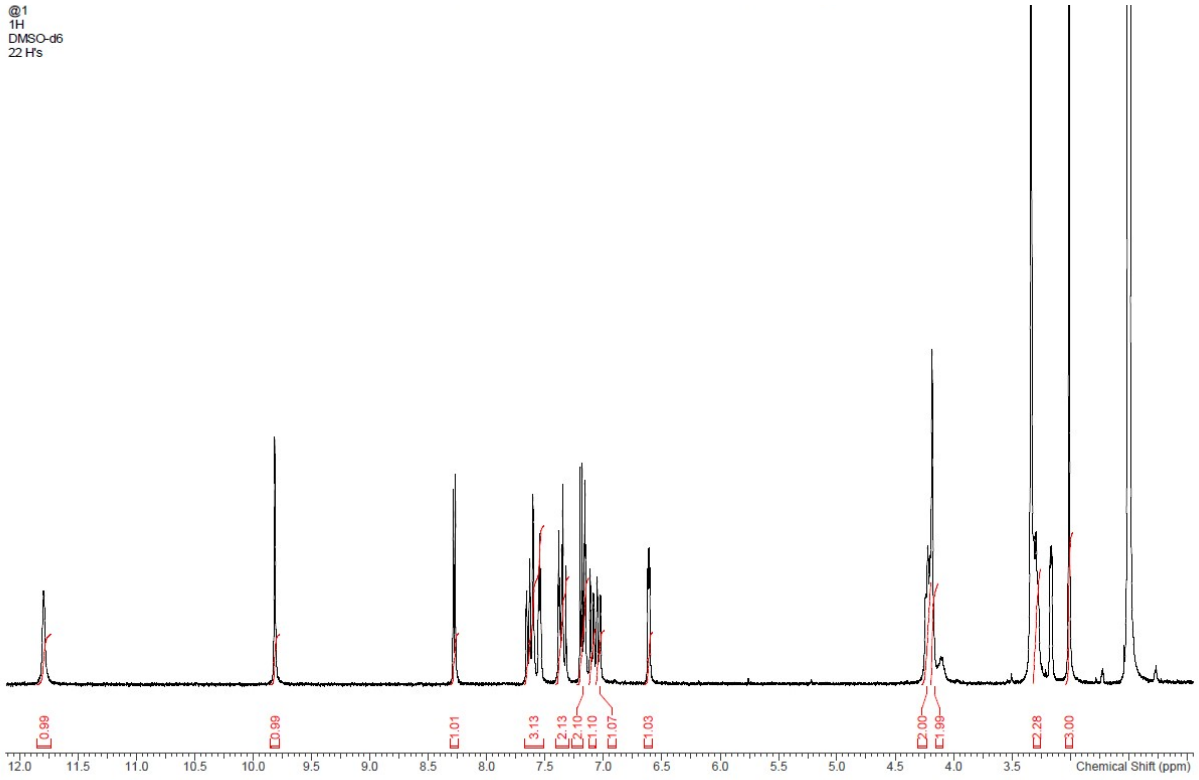

LC-MS (Method A)

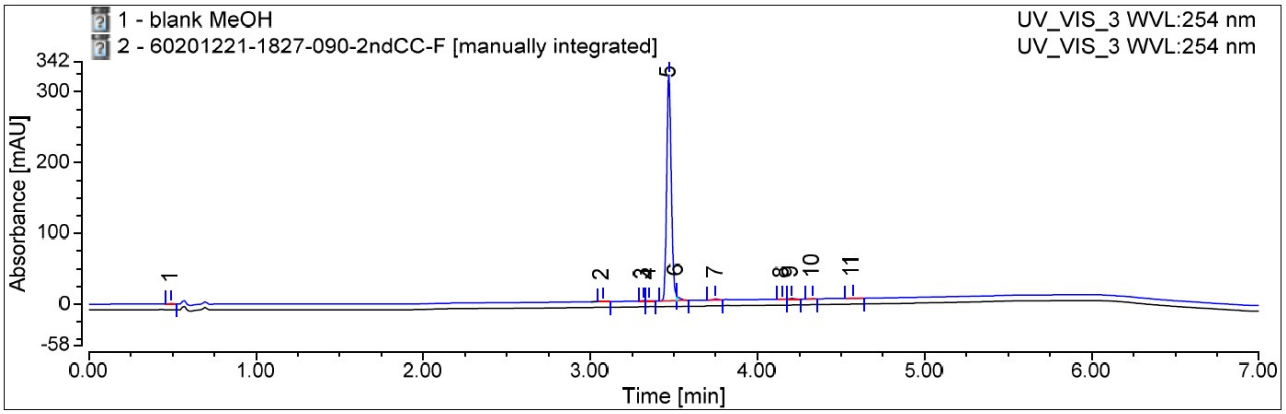

Purity (UV, 254nm): 96.9%

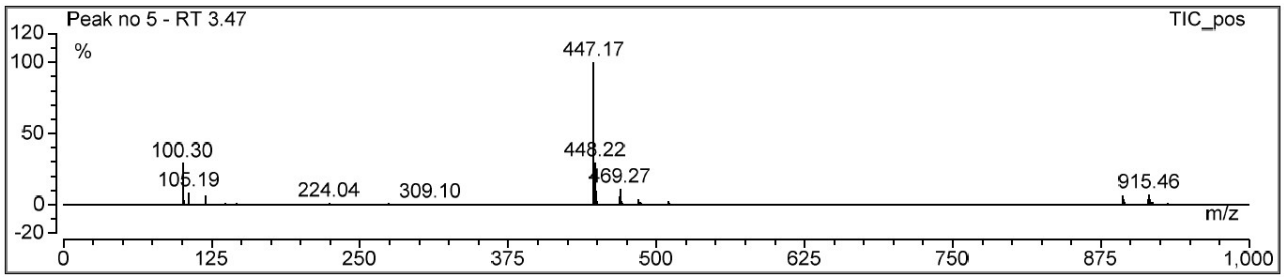
Peak no 5 - RT 3.47
TIC_pos
%
447.17
100.30
105.19
224.04
309.10
448.22
469.27
915.46
m/z
120
100
50
0
-20
0
125
250
375
500
625
750
875
1,000

3-phenyl-8-(1H-pyrrolo[2,3-b]pyridin-4-yl)-1,3,4,5-tetrahydro-2H-benzo[d]azepin-2-one (4).

^{1}H NMR (400 MHz, DMSO-*d6*)

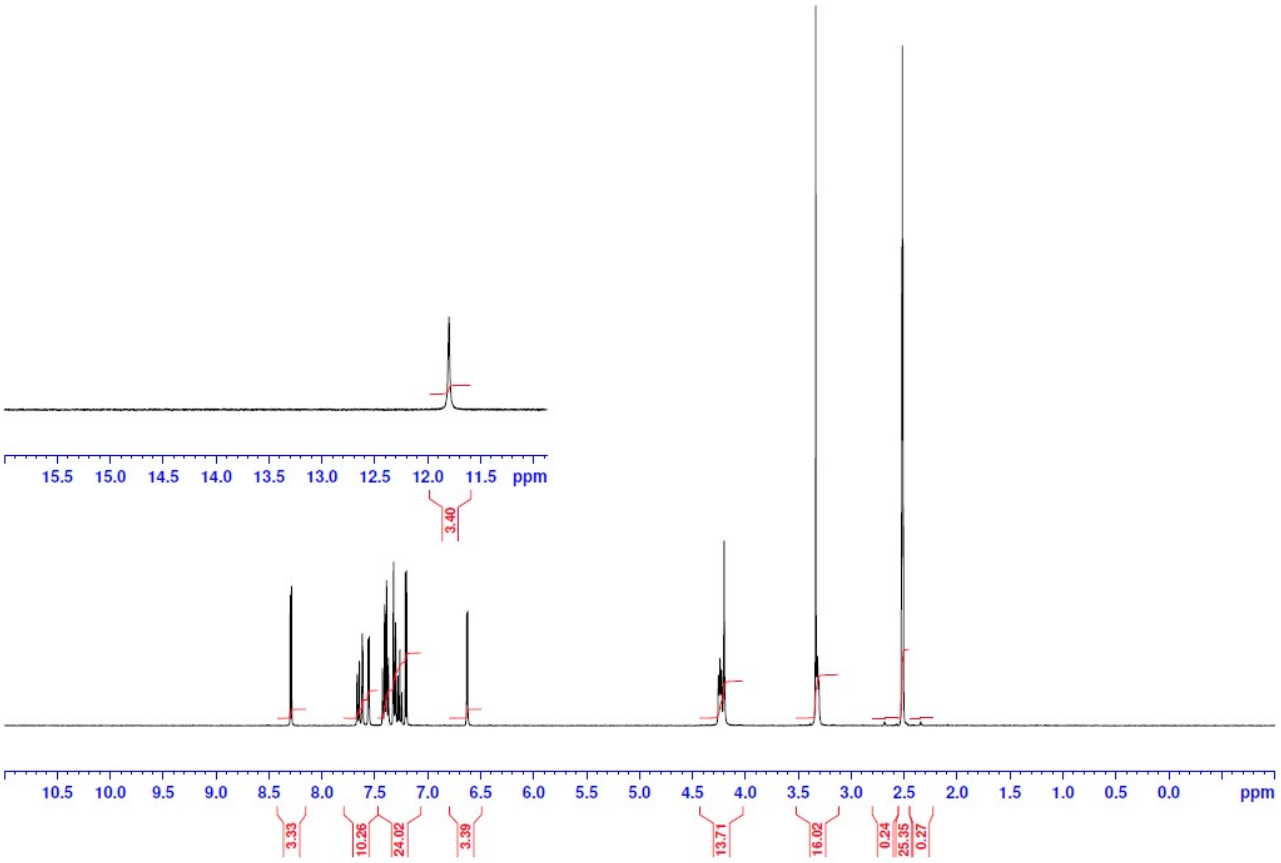

LC-MS (Method E)

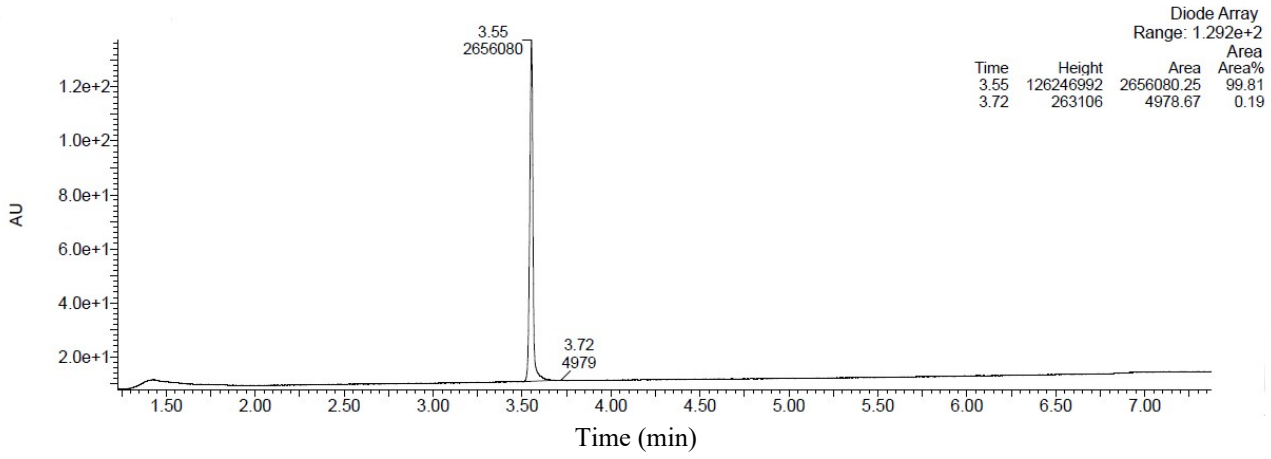

Purity (UV, DAD): 99.8%

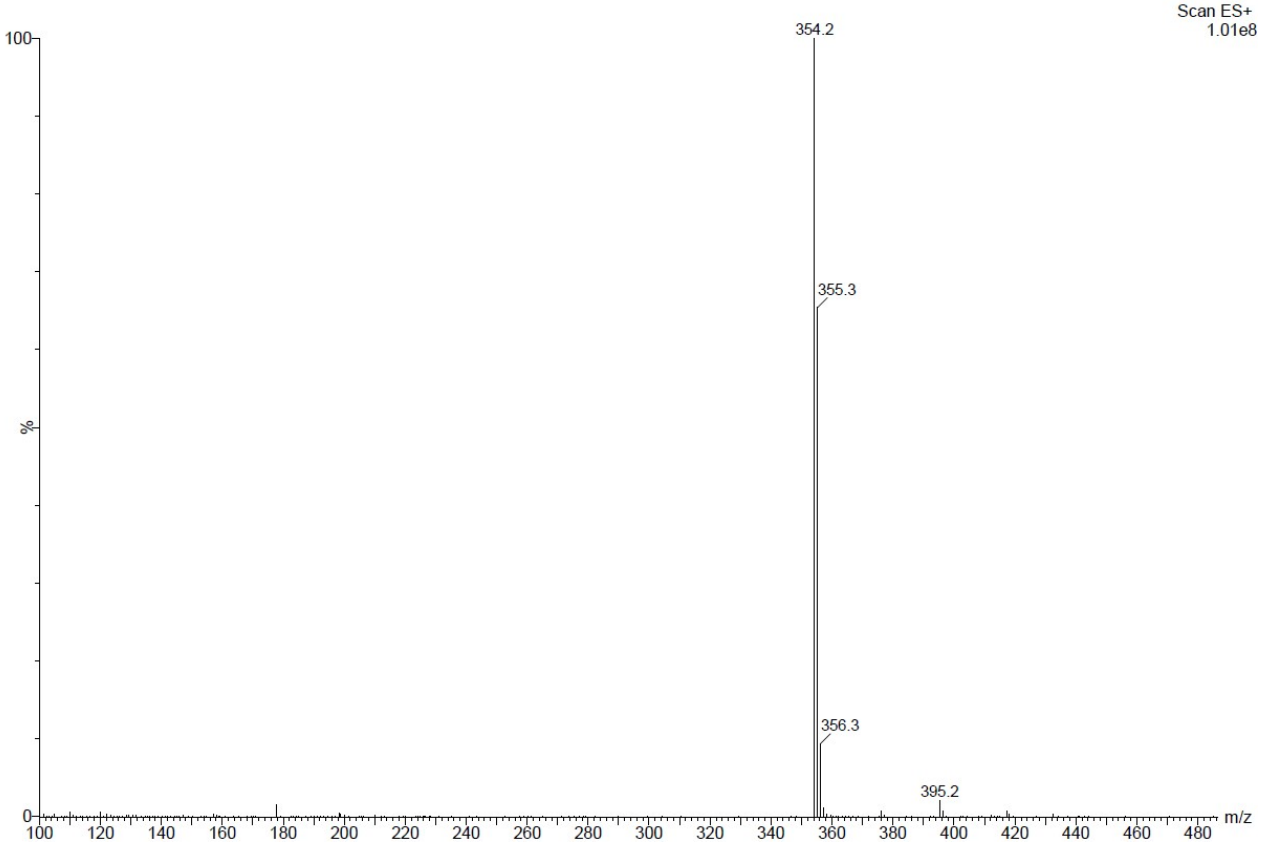

2-phenyl-8-(1H-pyrrolo[2,3-b]pyridin-4-yl)-1,2,4,5-tetrahydro-3H-benzo[c]azepin-3-one (5).

^{1}H NMR (400 MHz, DMSO-*d6*)

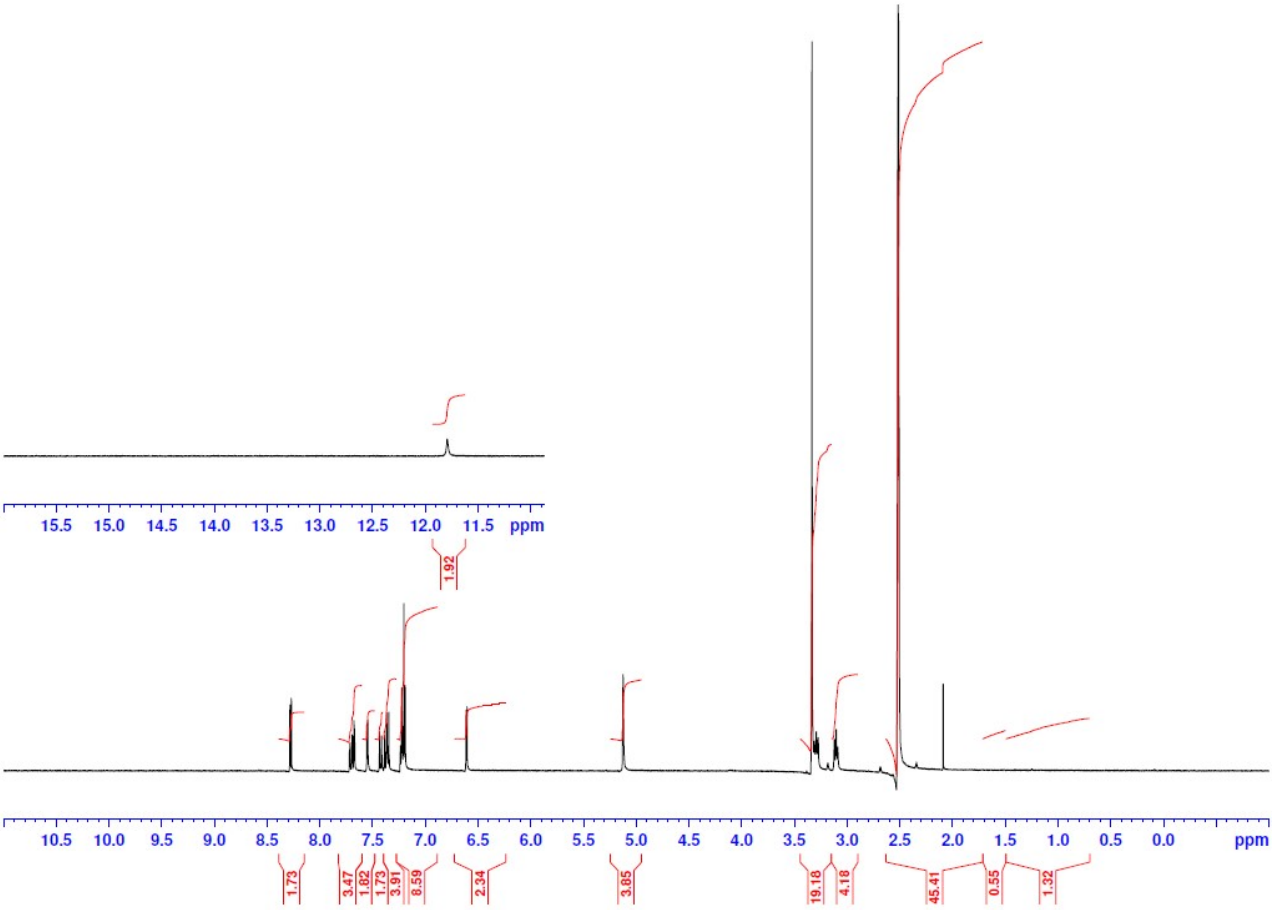

LC-MS (Method E)

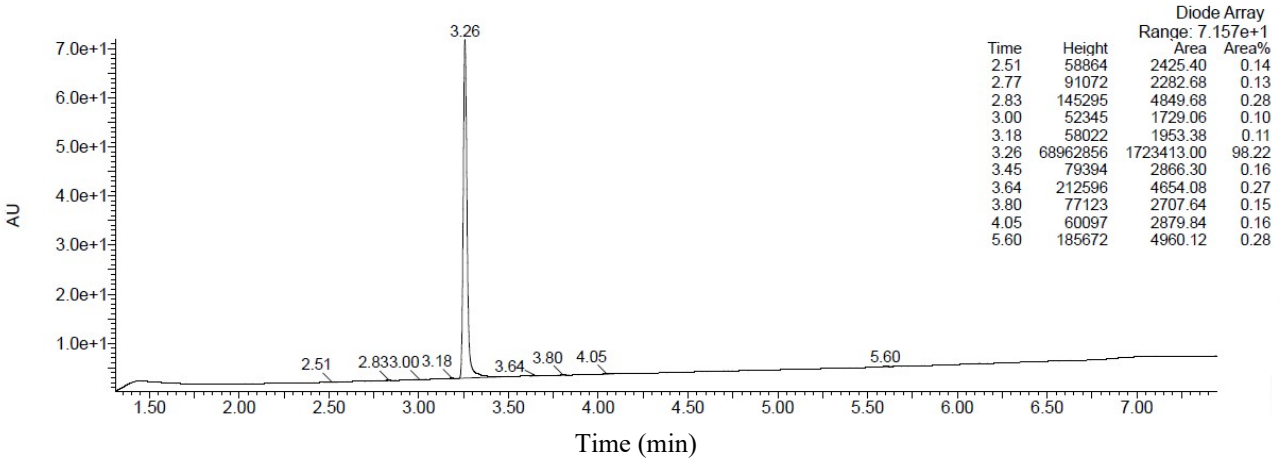

Purity (UV, DAD): 98.2%

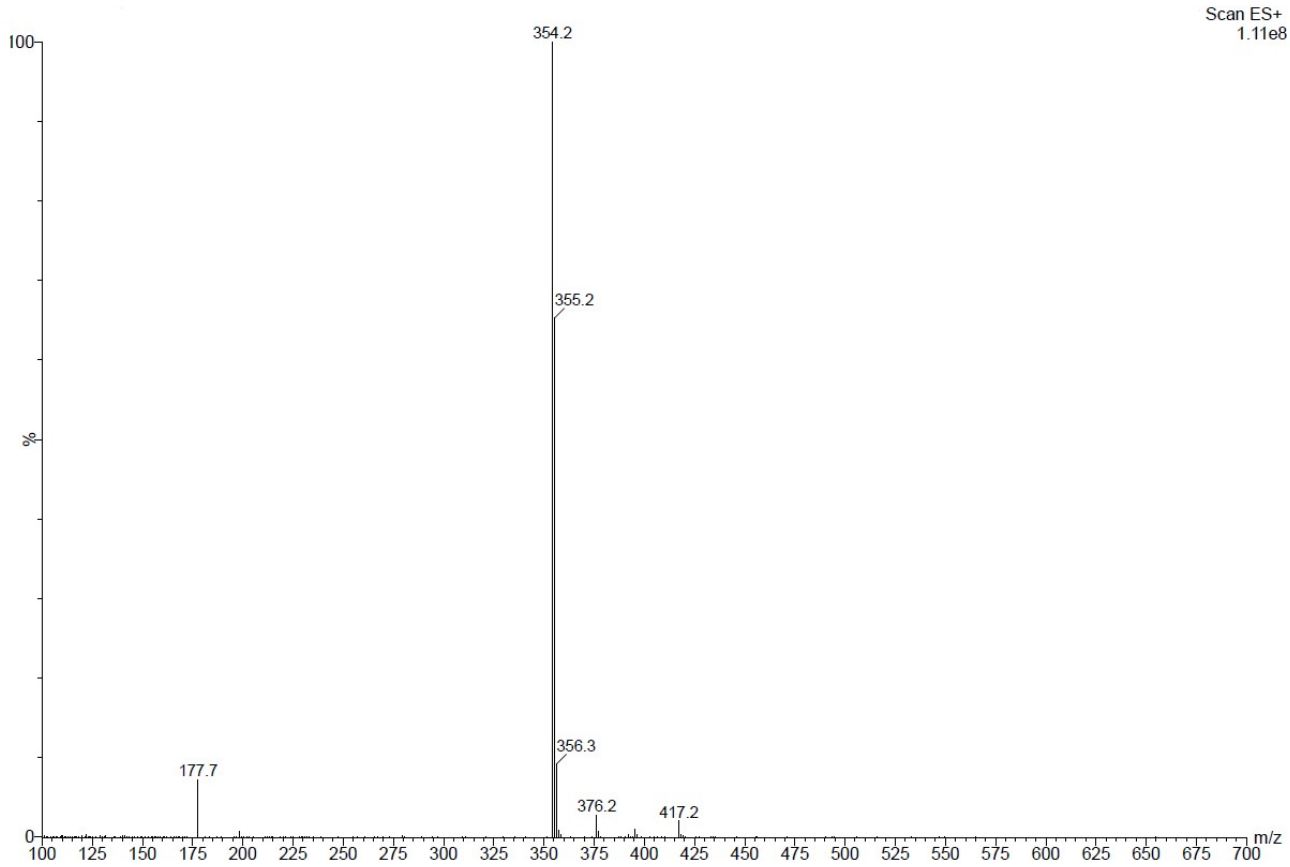
Scan ES+
1.11e8
100
%
0
354.2
355.2
356.3
177.7
376.2
417.2
m/z
100 125 150 175 200 225 250 275 300 325 350 375 400 425 450 475 500 525 550 575 600 625 650 675 700

3-phenyl-8-(7H-pyrrolo[2,3-d]pyrimidin-4-yl)-1,3,4,5-tetrahydro-2H-benzo[d]azepin-2-one (6).

^{1}H NMR (300MHz, CD_3OD)

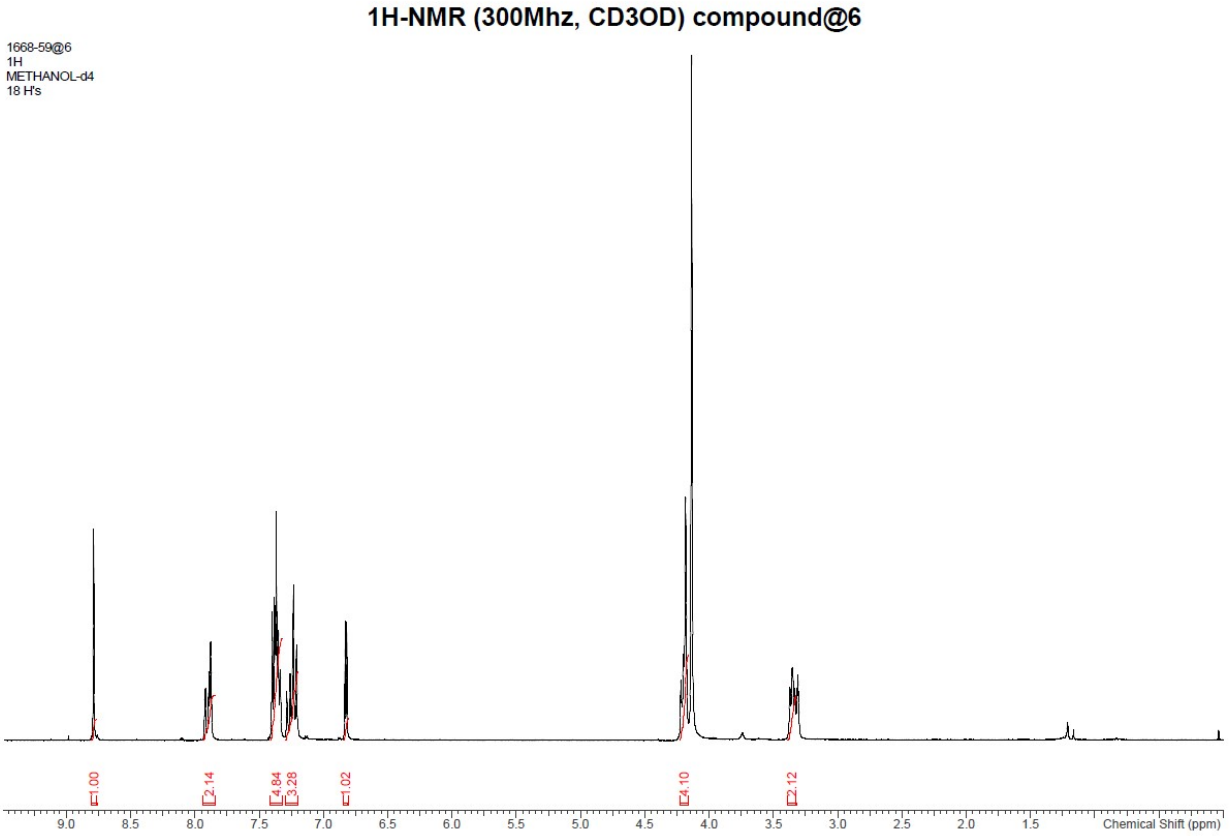

LC-MS(Method C)

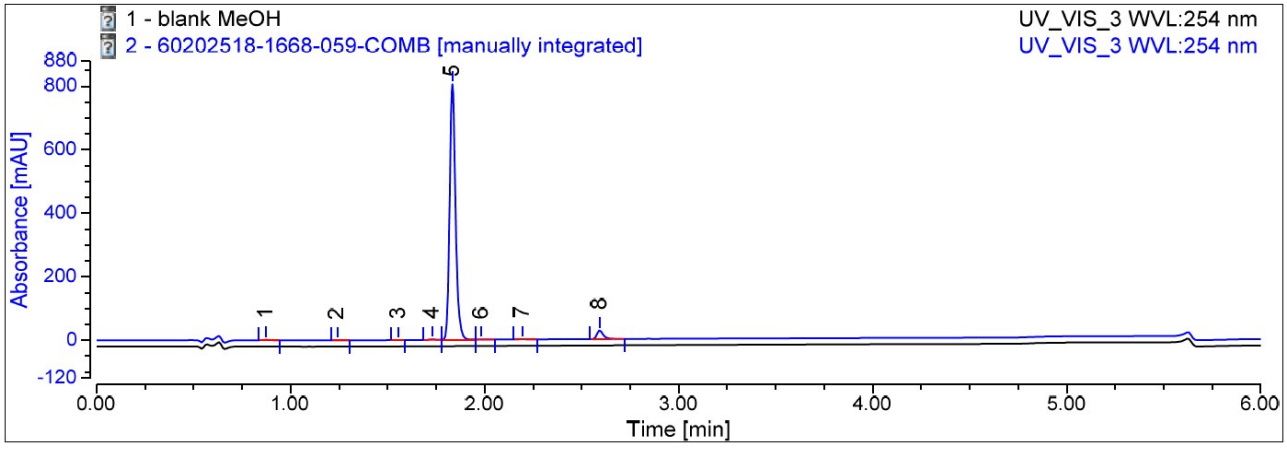

Purity (UV, 254nm): 96.8%

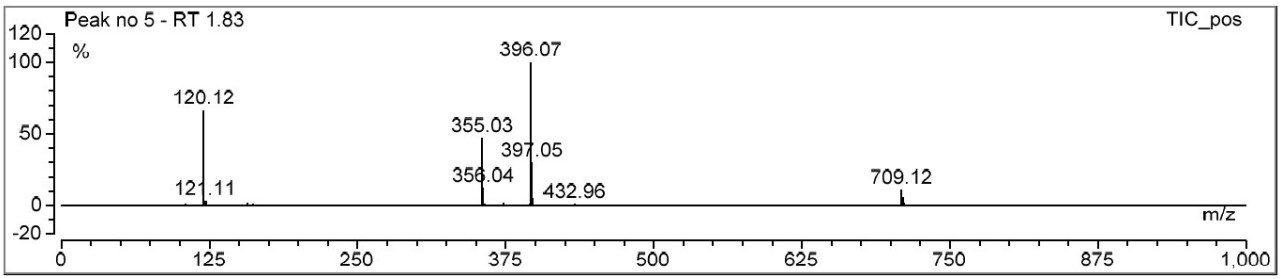

8-(3-methyl-1H-pyrrolo[2,3-b]pyridin-4-yl)-3-phenyl-1,3,4,5-tetrahydro-2H-benzo[d]azepin-2-one (7).

^{1}H NMR (400 MHz, DMSO-*d6*)

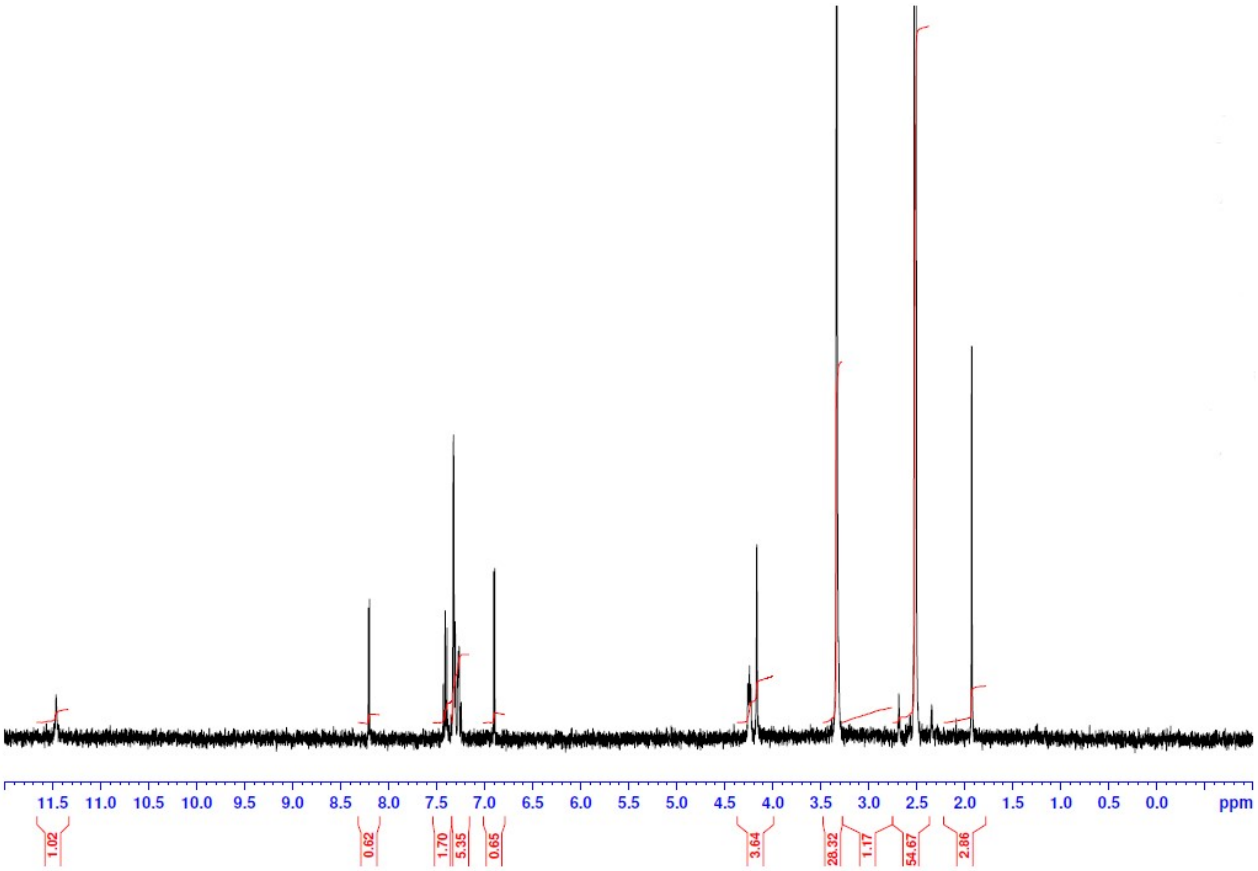

LC-MS (Method E)

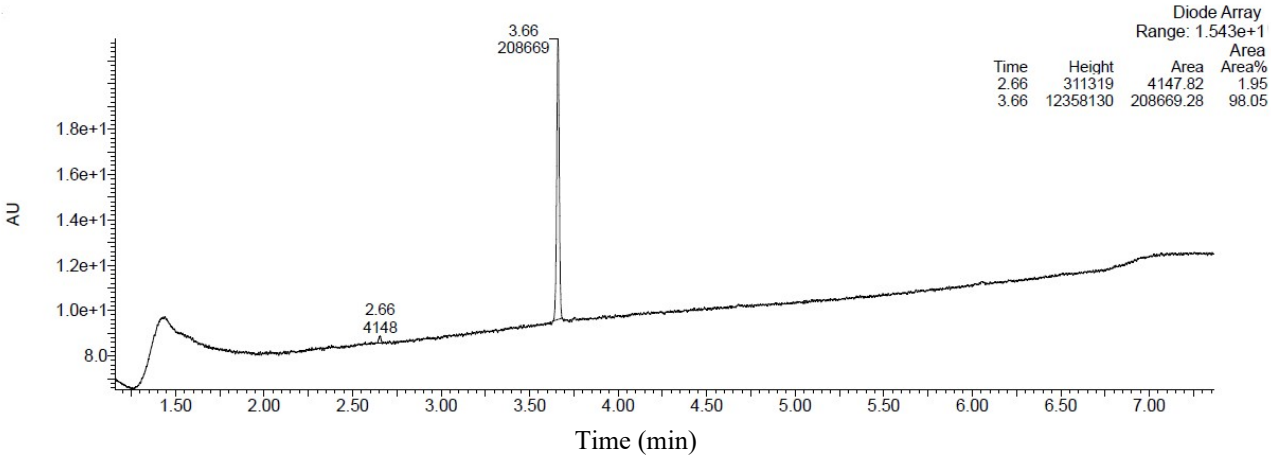

Purity (UV, DAD): 98.1%

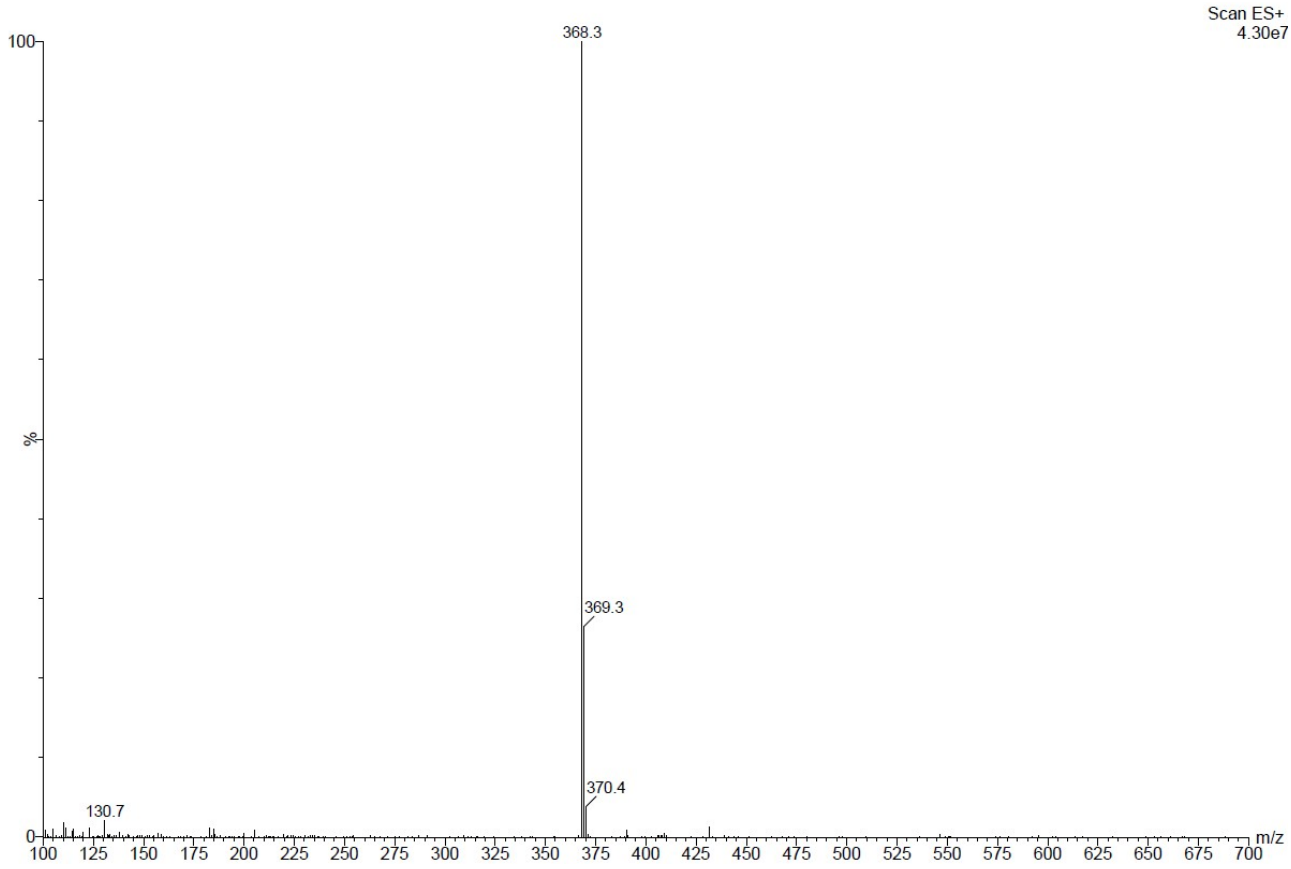
Scan ES+
4.30e7
100
%
0
368.3
369.3
370.4
130.7
100 125 150 175 200 225 250 275 300 325 350 375 400 425 450 475 500 525 550 575 600 625 650 675 700
m/z

3-phenyl-8-(pyridin-4-yl)-1,3,4,5-tetrahydro-2H-benzo[d]azepin-2-one (8).

^{1}H NMR (400 MHz, $CDCl_3$)

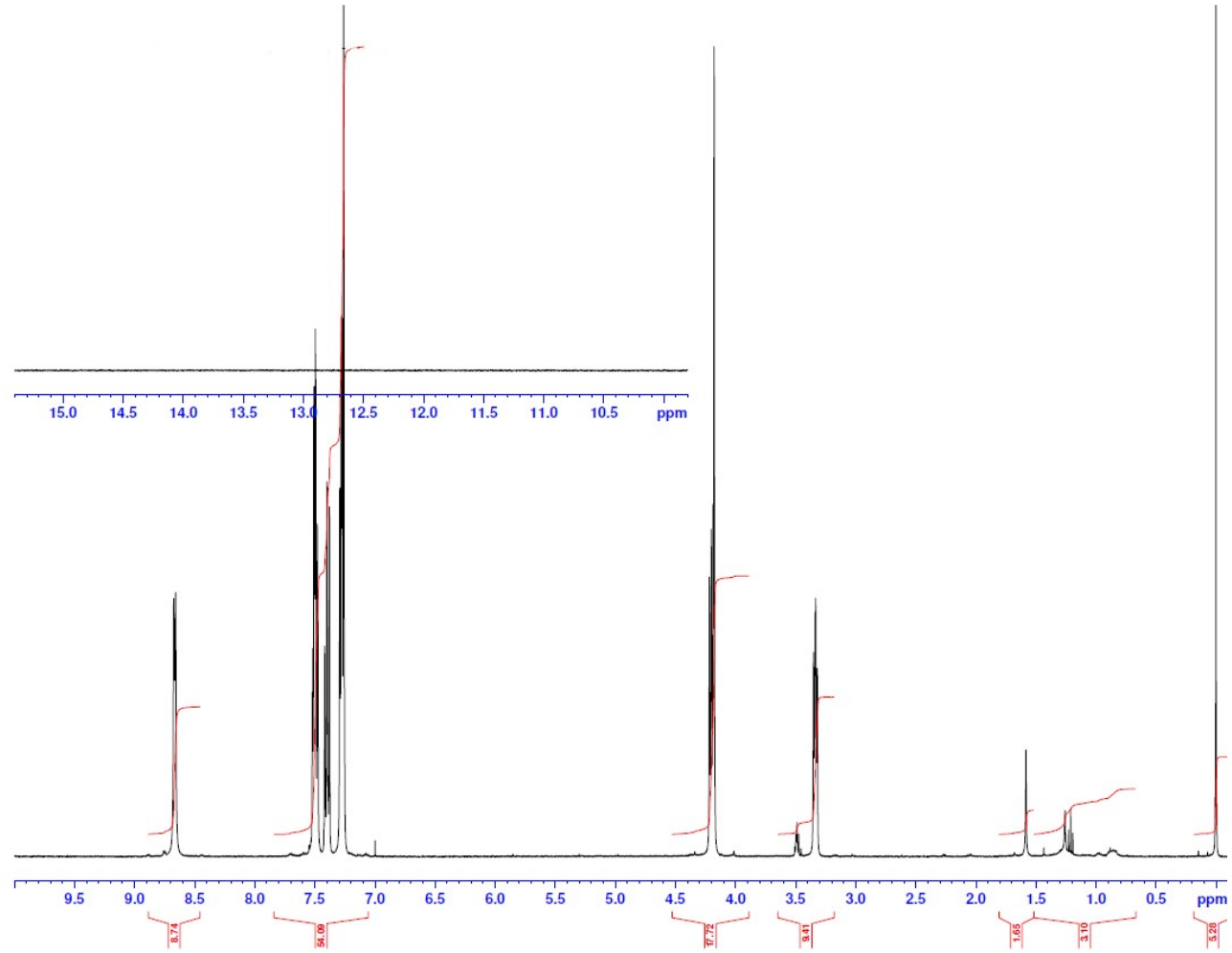

LC-MS (Method F)

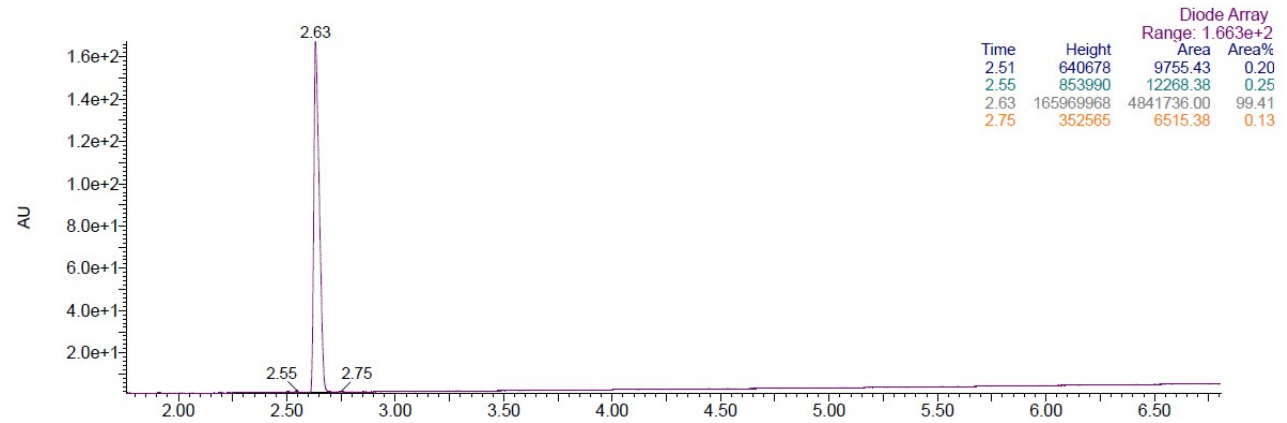

Purity (UV, DAD): 99.4%

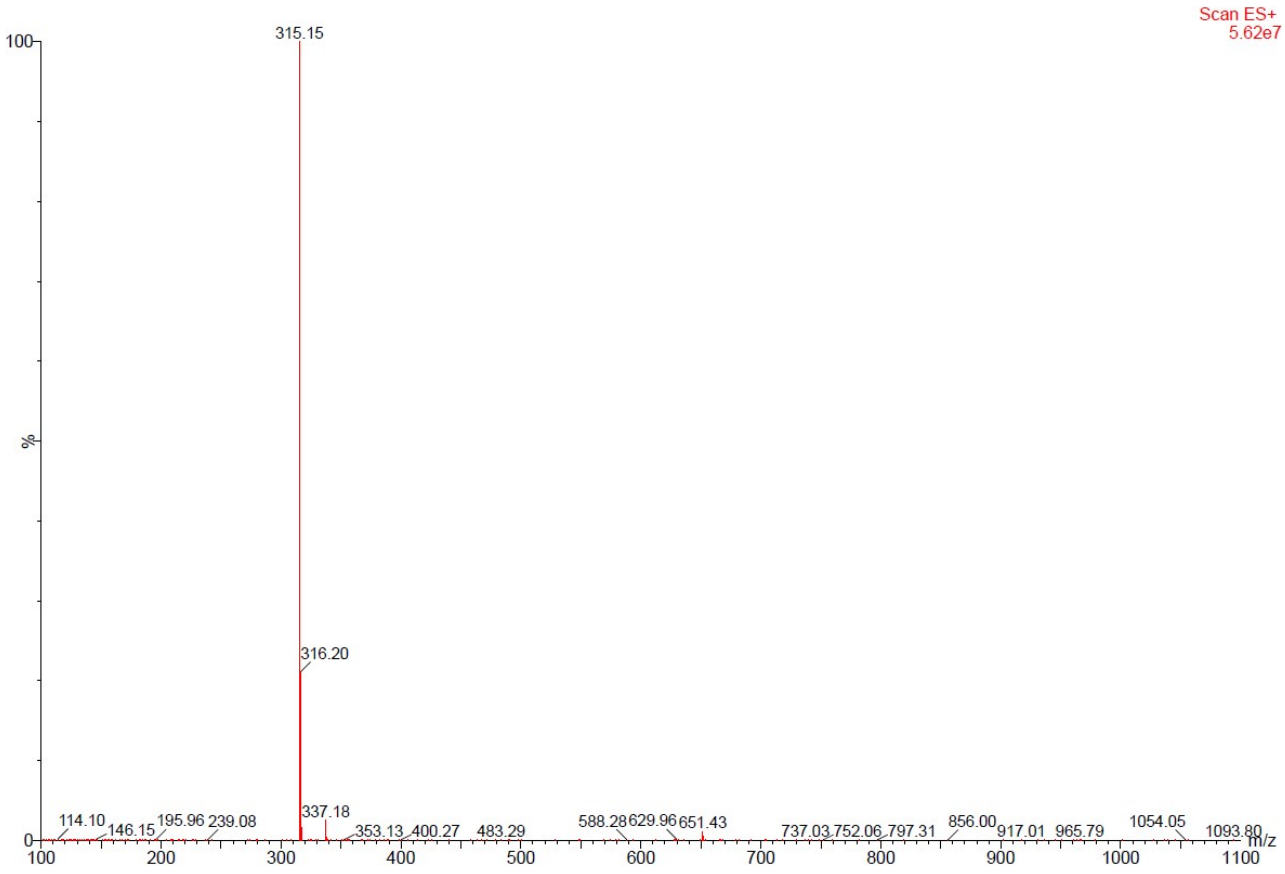

8-(2-aminopyridin-4-yl)-3-phenyl-1,3,4,5-tetrahydro-2H-benzo[d]azepin-2-one (9).

^{1}H NMR (300MHz, DMSO-*d6*)

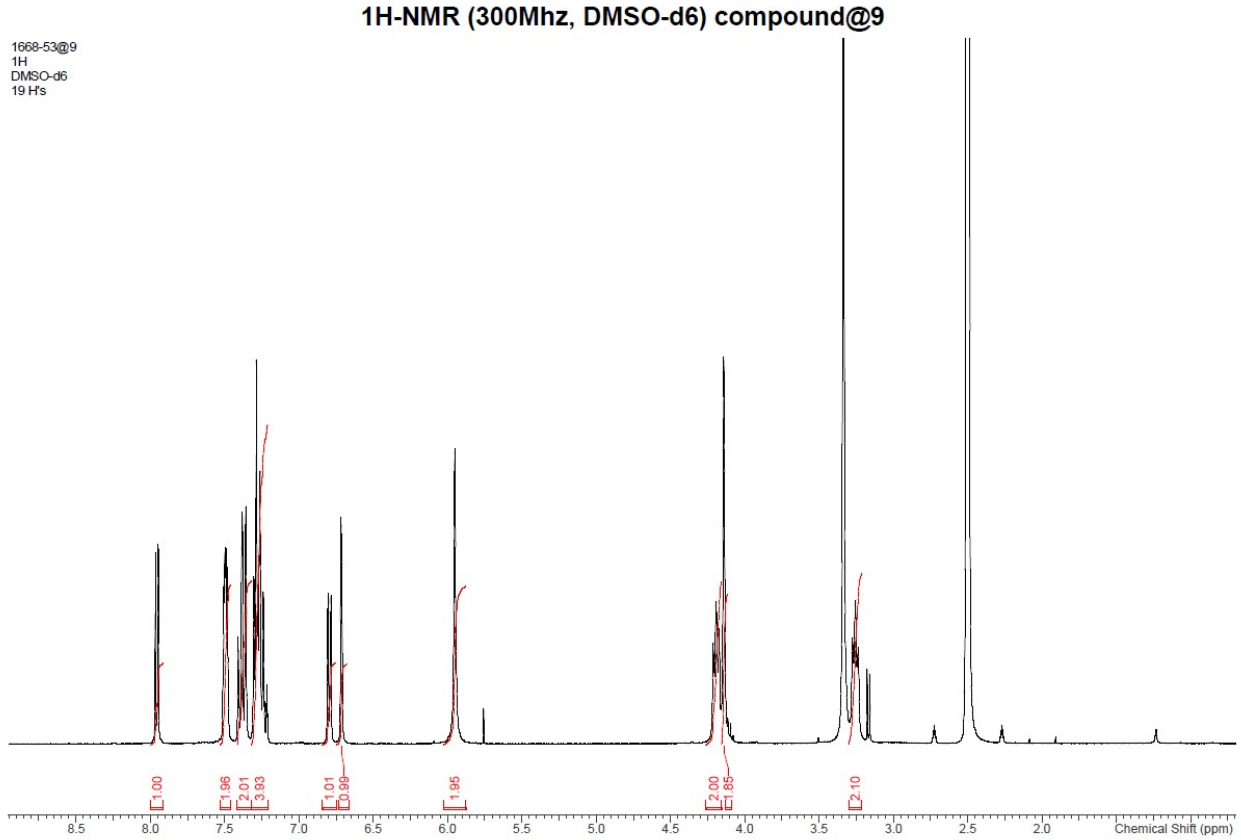

LC-MS(Method C)

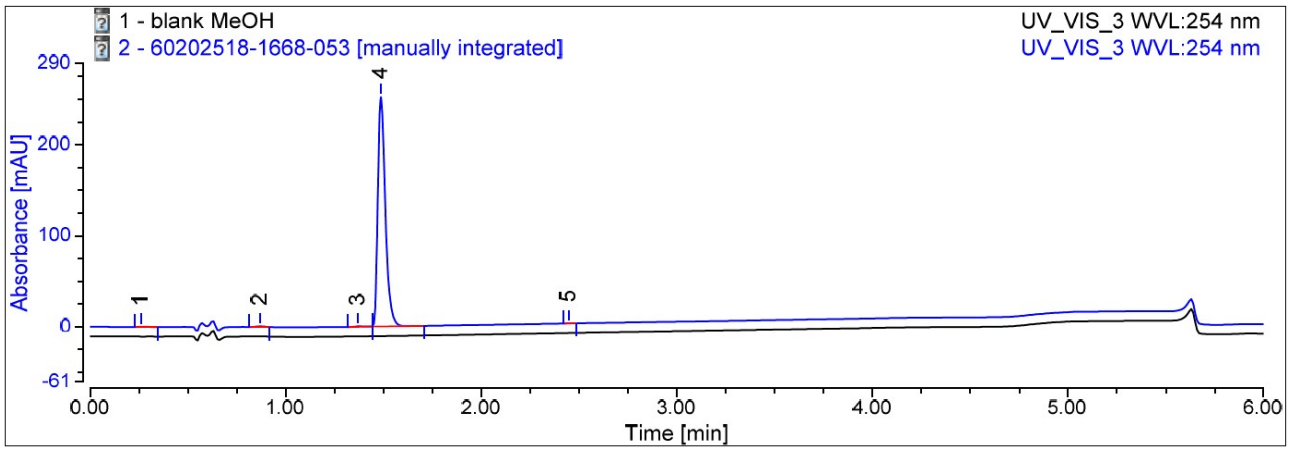

Purity (UV, 254nm): 99.3%

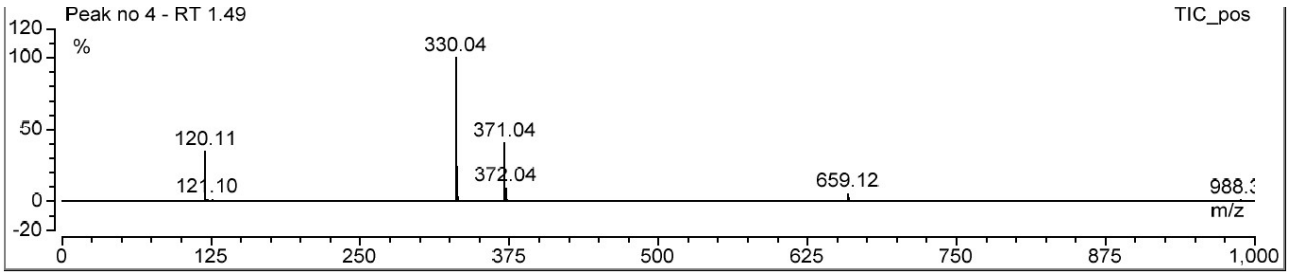

3-phenyl-8-(1H-pyrazol-4-yl)-1,3,4,5-tetrahydro-2H-benzo[d]azepin-2-one (10).

^{1}H NMR (300MHz, CD_3OD)

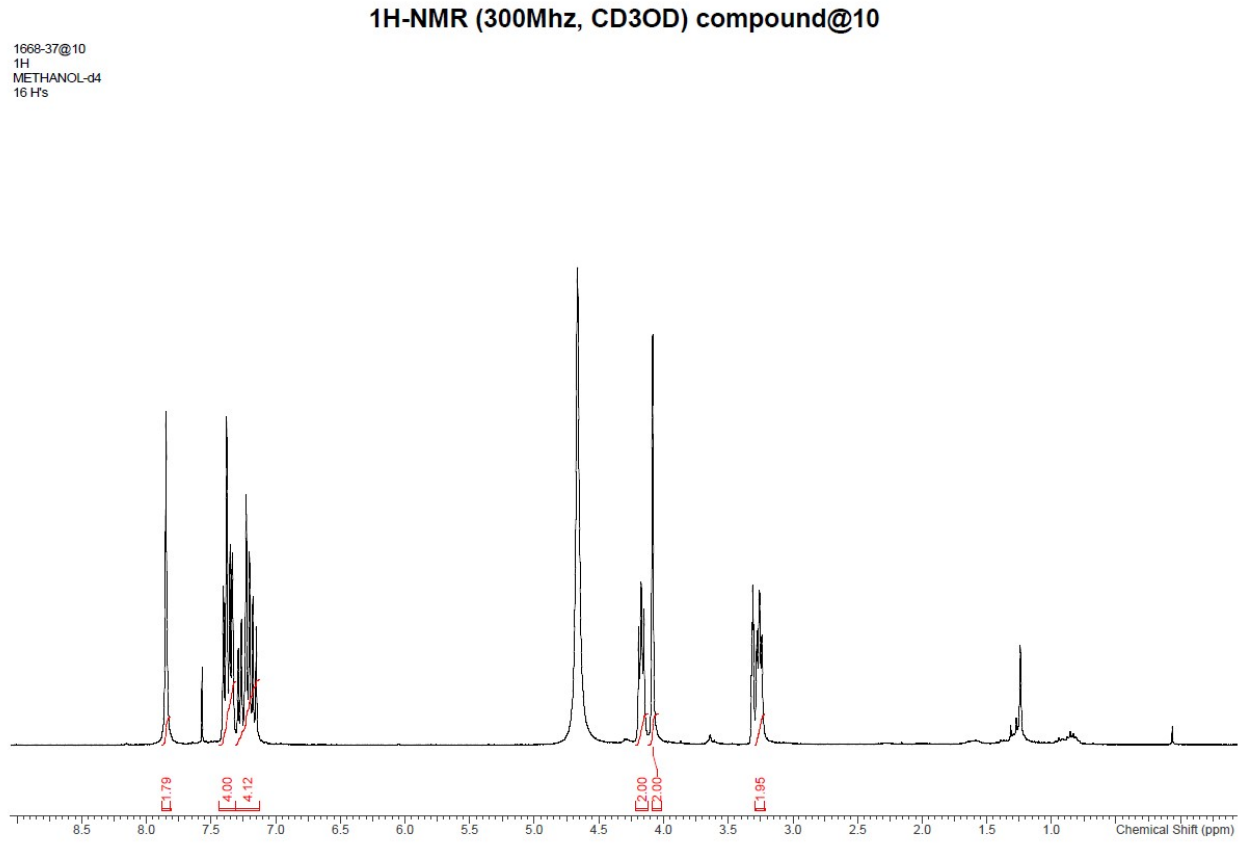

LC-MS(Method C)

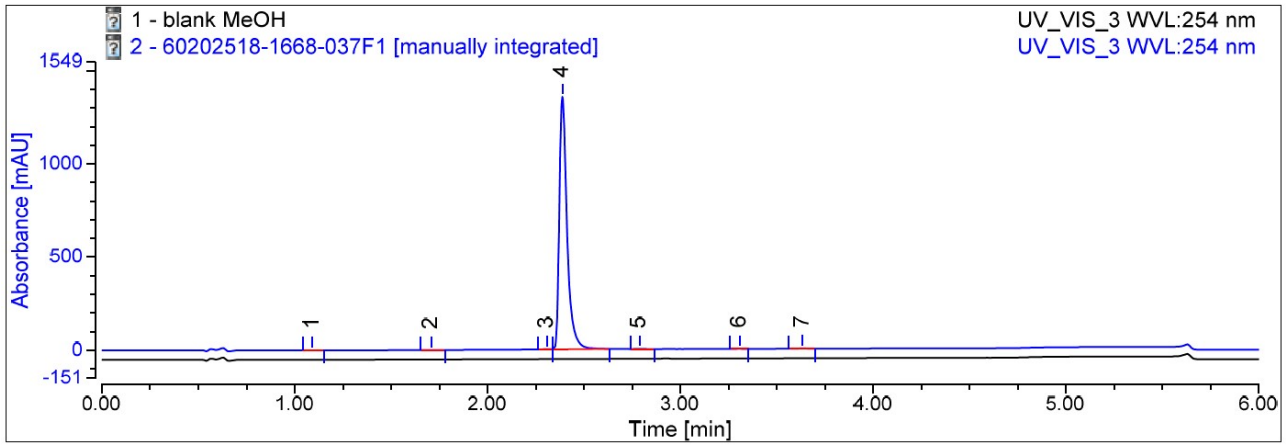

Purity (UV, 254nm): 99.6%

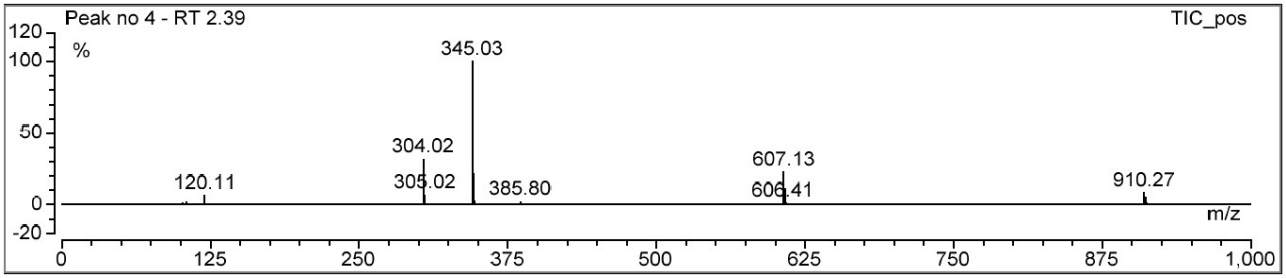

8-(1H-indazol-5-yl)-3-phenyl-1,3,4,5-tetrahydro-2H-benzo[d]azepin-2-one (11).

^{1}H NMR (300MHz, CD_3OD)

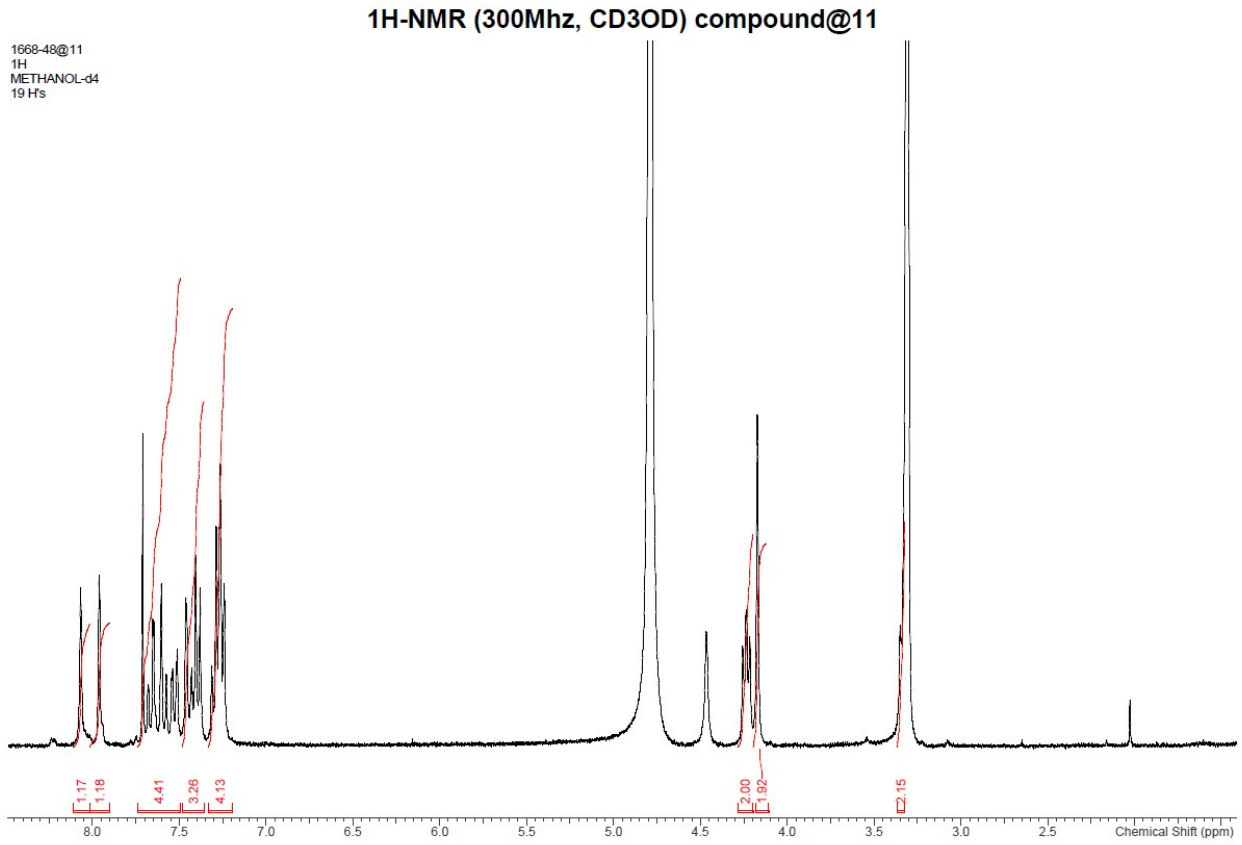

LC-MS(Method C)

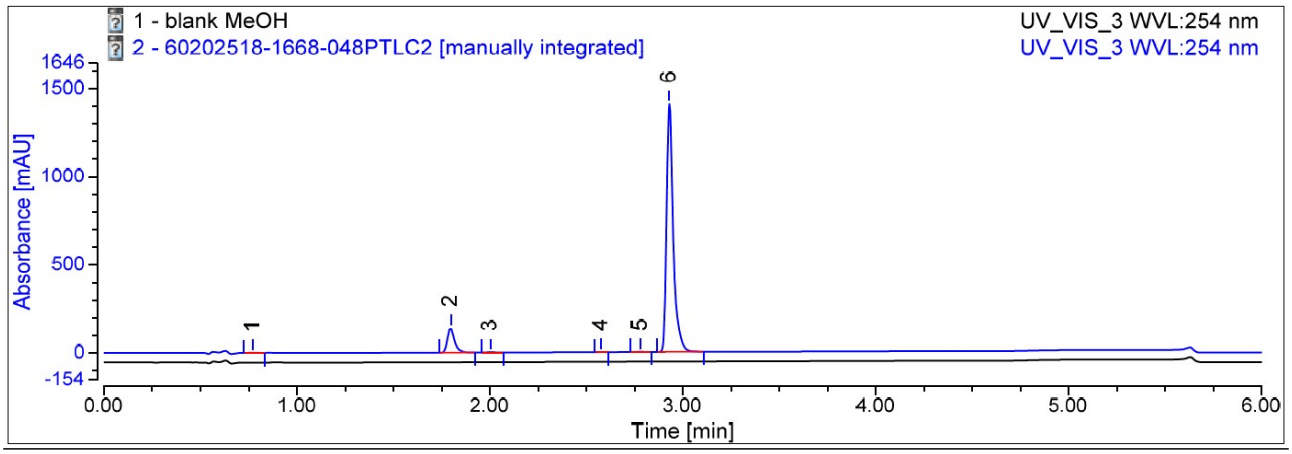

Purity (UV, 254nm): 90.1%

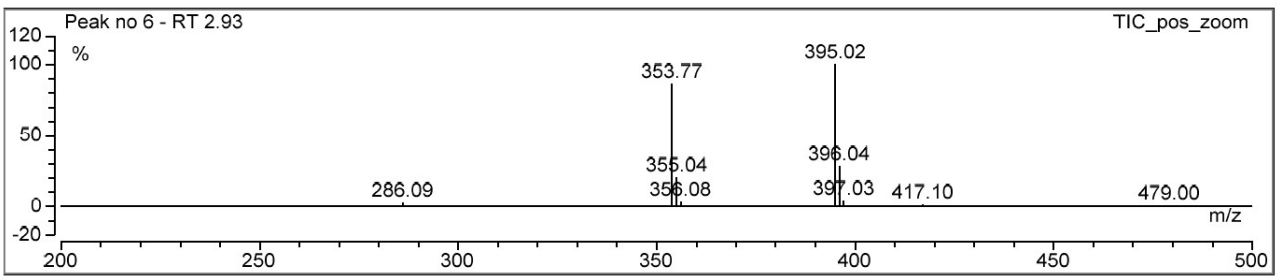

3-methyl-8-(1H-pyrrolo[2,3-b]pyridin-4-yl)-1,3,4,5-tetrahydro-2H-benzo[d]azepin-2-onen (12)

^{1}H NMR (300MHz, CD_3OD)

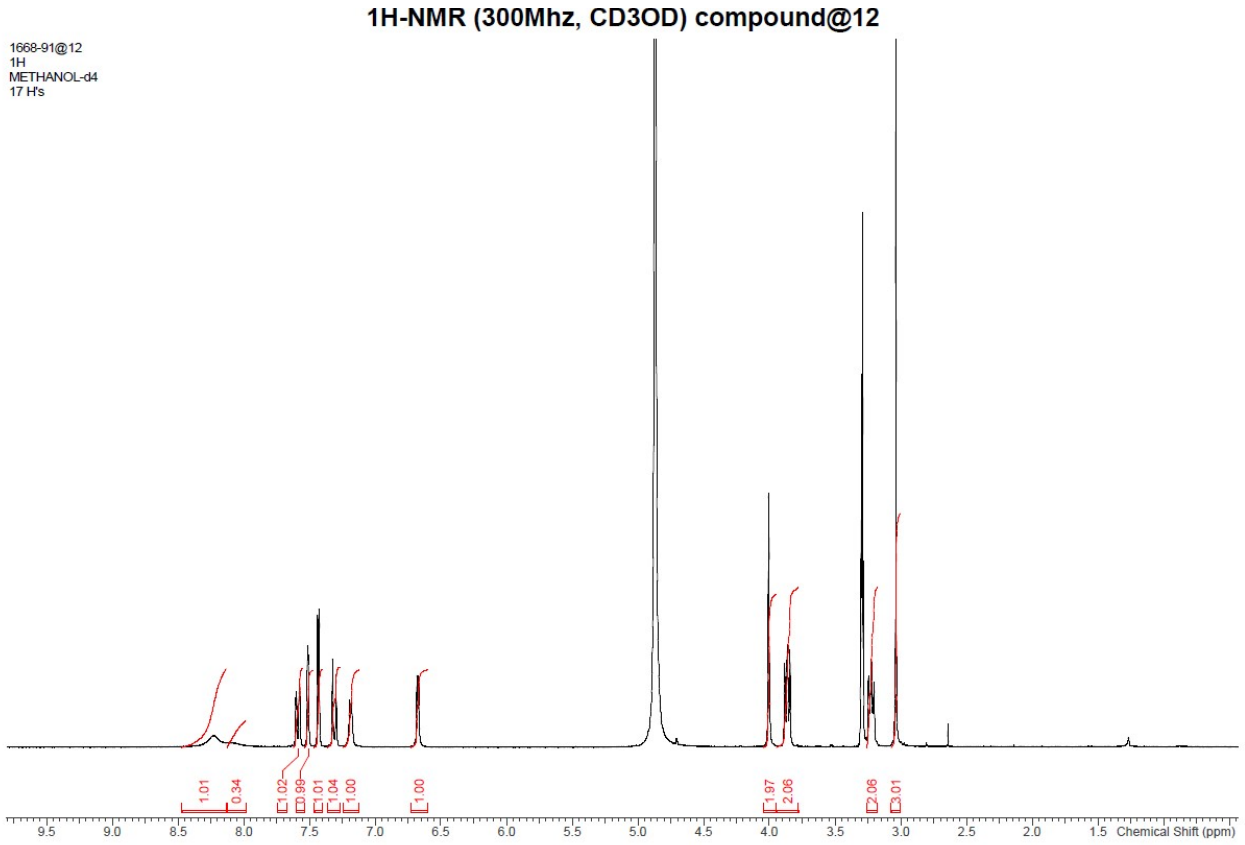

LC-MS(Method B)

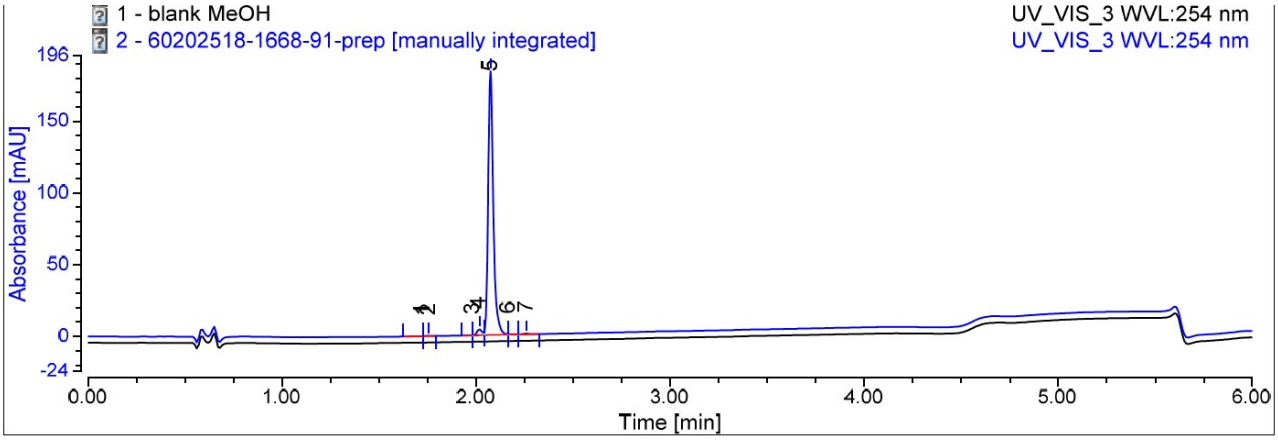

Purity (UV, 254nm): 97.2%

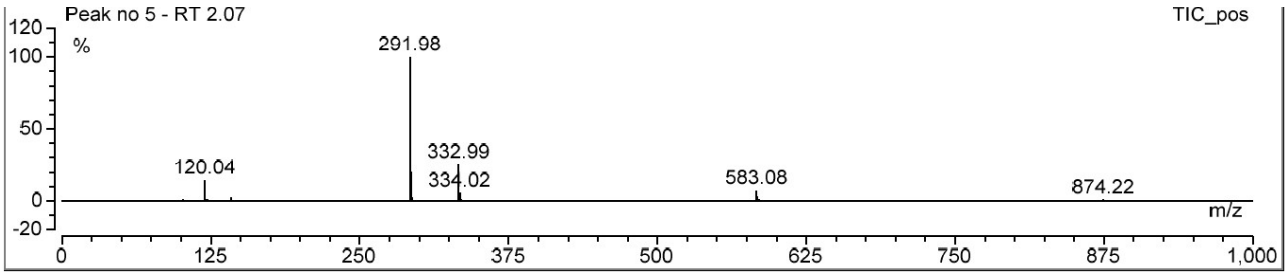

3-(2-morpholinoethyl)-8-(1H-pyrrolo[2,3-b]pyridin-4-yl)-1,3,4,5-tetrahydro-2H-benzo[d]azepin-2-one (13).

^{1}H NMR (300MHz, CD_3OD)

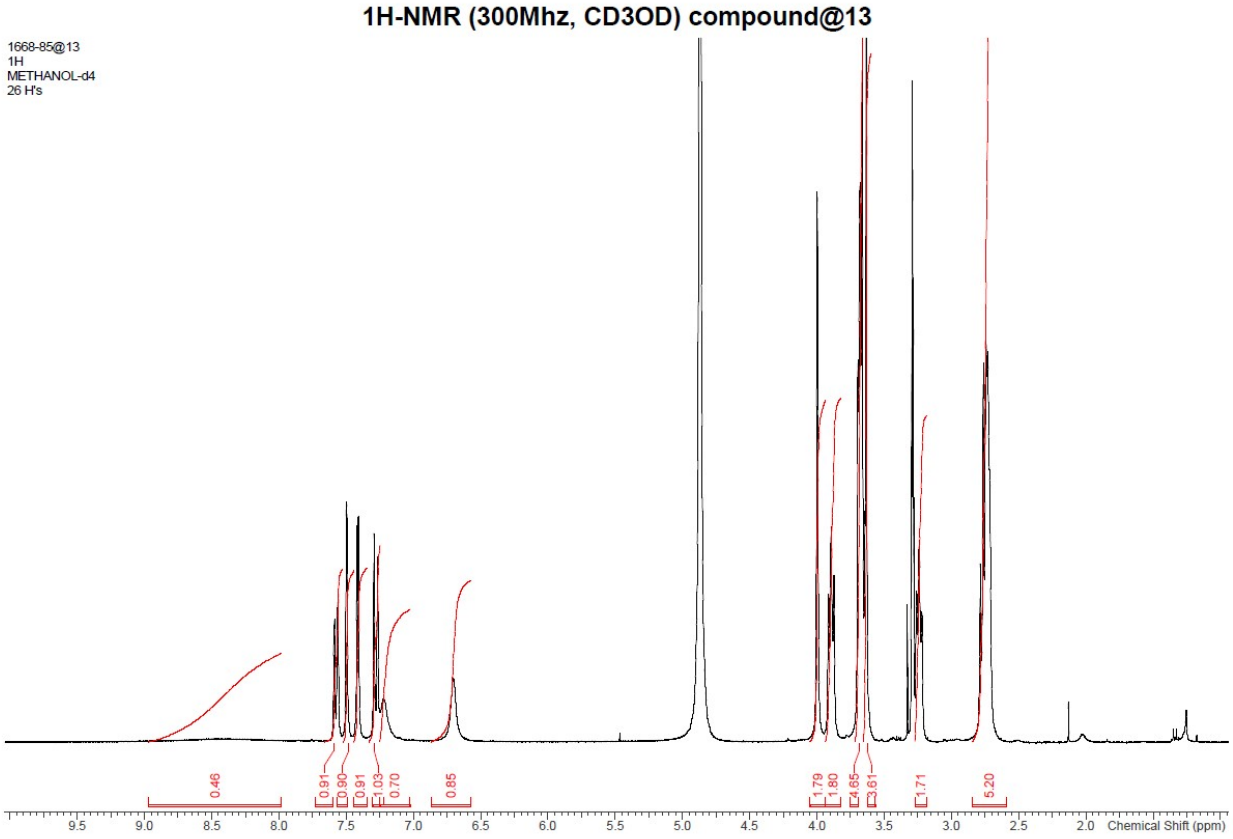

LC-MS(Method A)

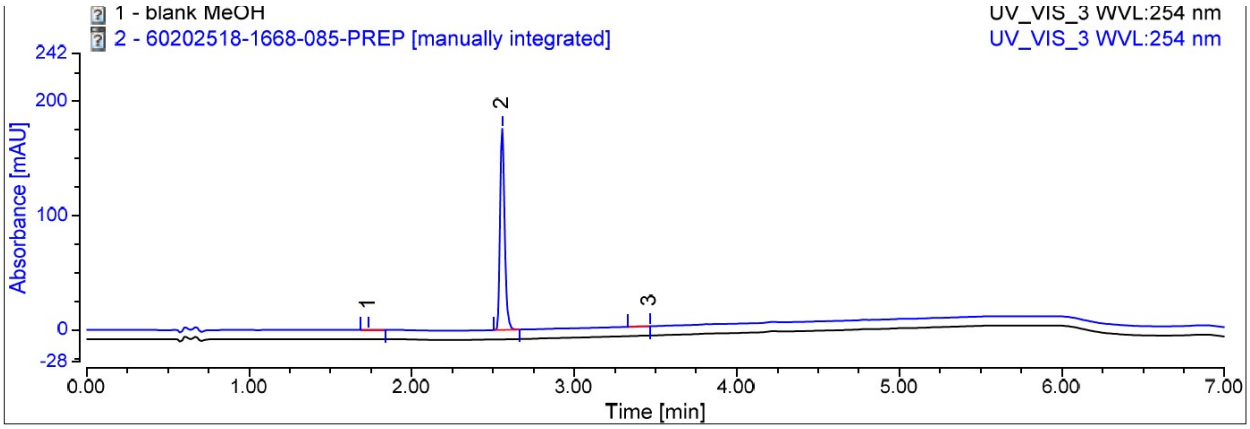

Purity (UV, 254nm): 99.8%

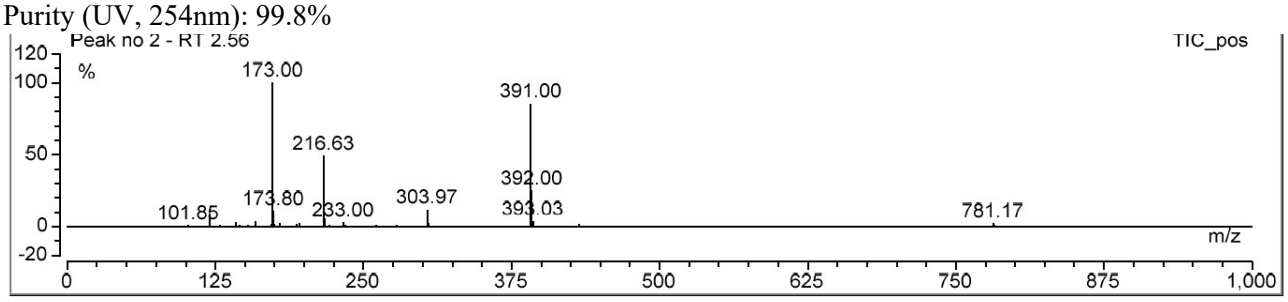

3-(3-methoxyphenyl)-8-(1H-pyrrolo[2,3-b]pyridin-4-yl)-1,3,4,5-tetrahydro-2H-benzo[d]azepin-2-one (14).

^{1}H NMR (300MHz, DMSO-*d6*)

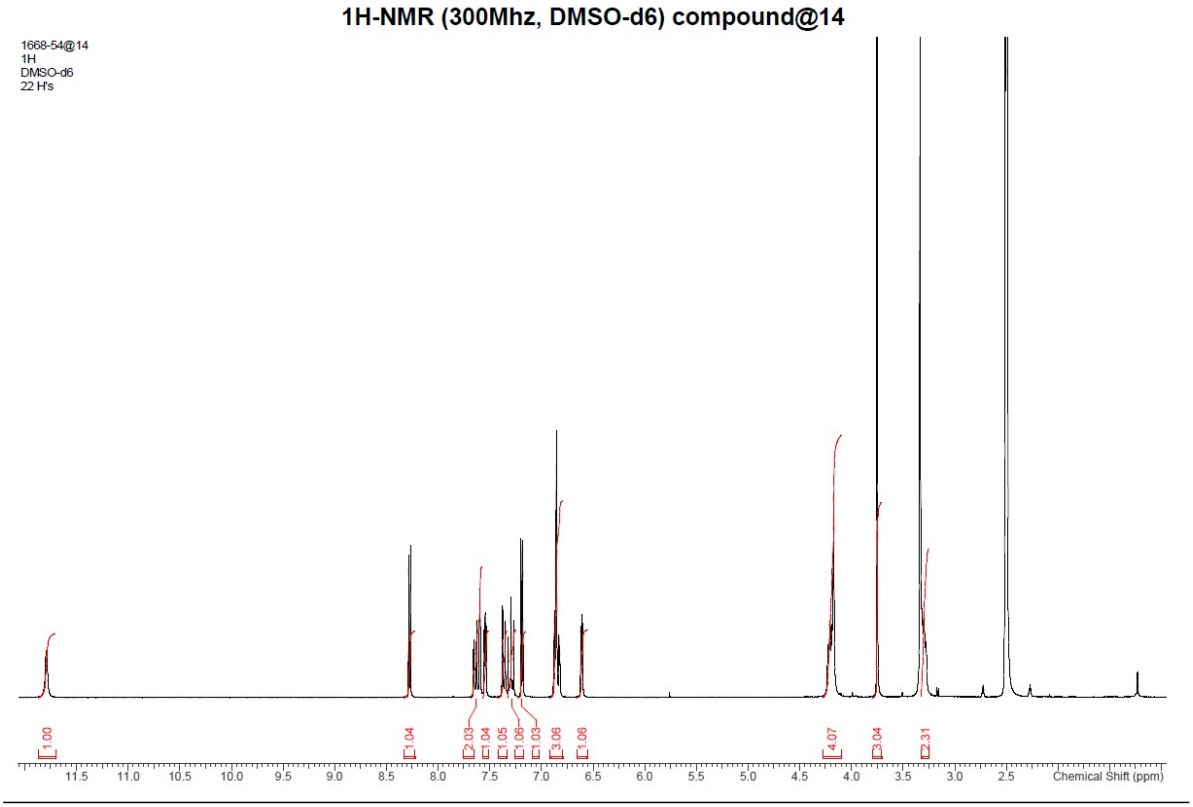

LC-MS(Method C)

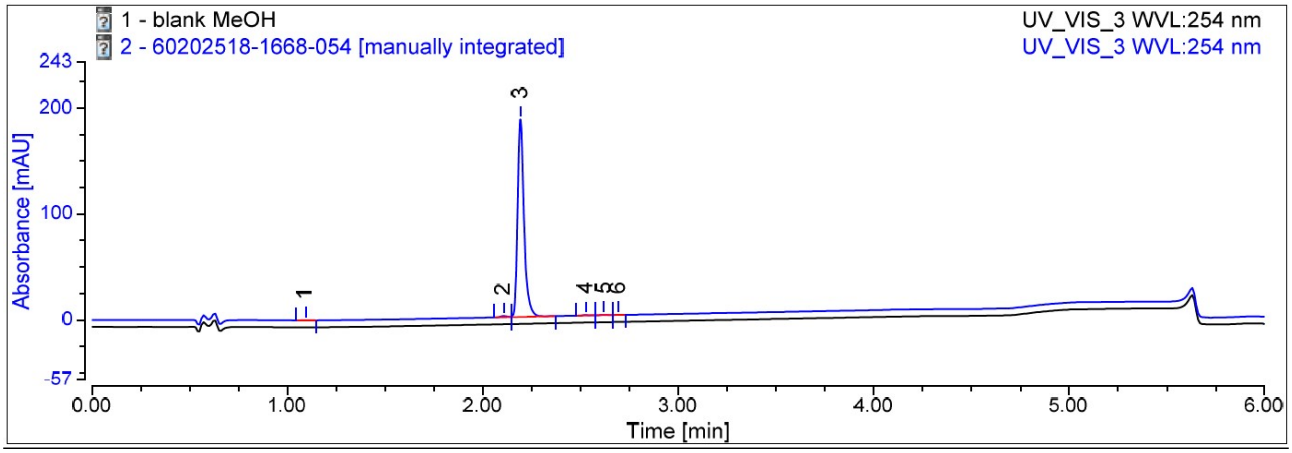

Purity (UV, 254nm): 98.8%

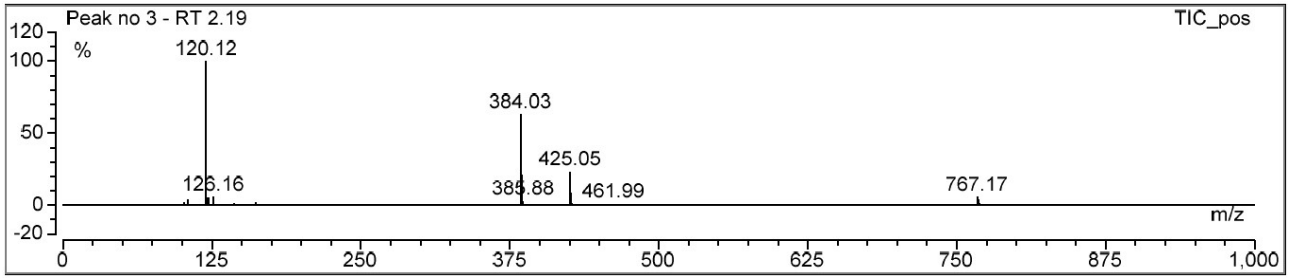

3-(3-(3-(4-methylpiperazin-1-yl)propoxy)phenyl)-8-(1H-pyrrolo[2,3-b]pyridin-4-yl)-1,3,4,5-tetrahydro-2H-benzo[d]azepin-2-one (15).

^{1}H NMR (300MHz, DMSO-*d6*)

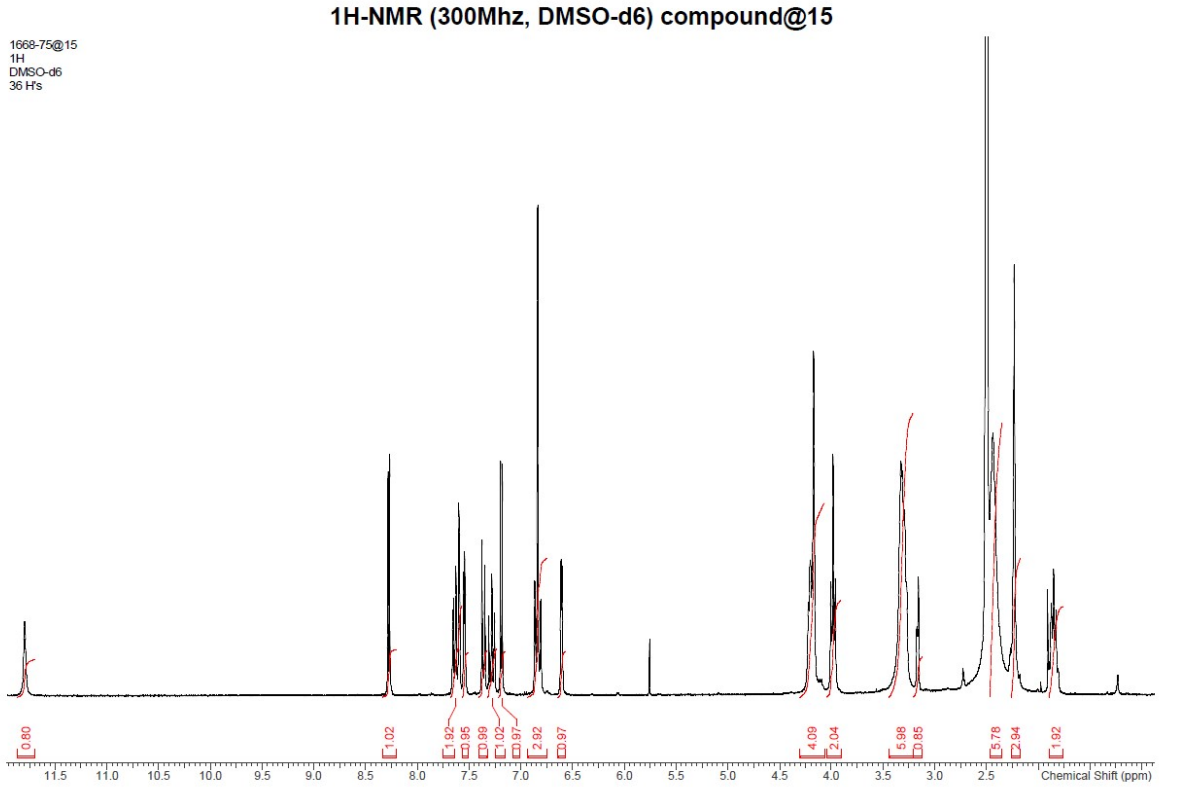

LC-MS (Method D)

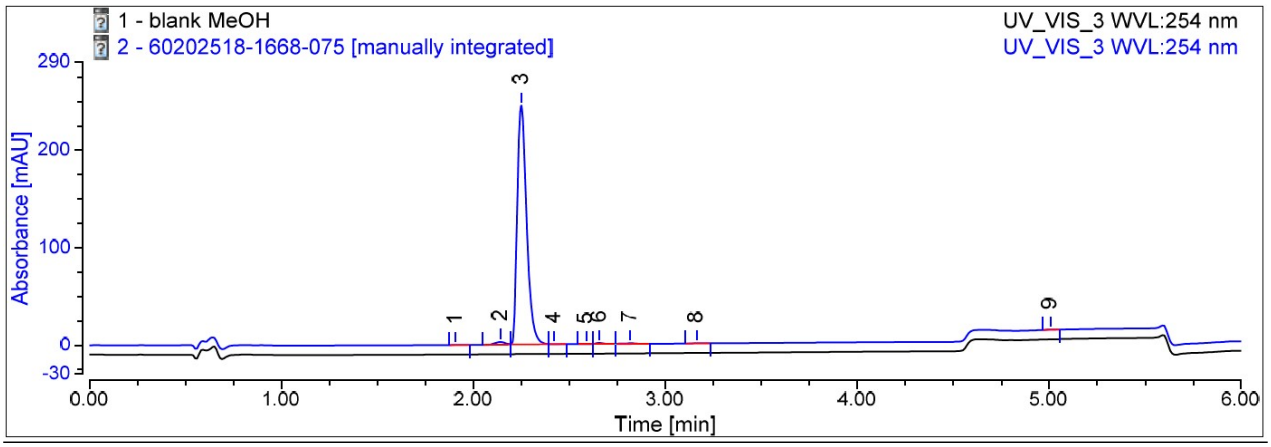

Purity (UV, 254nm): 97.6%